NASA CR-159528




National Aeronautics and Space Administration

# DEFINITION OF SMOLDER EXPERIMENTS FOR SPACELAB

*PRINCETON COMBUSTION RESEARCH LABORATORIES, INC.*

*1041 U.S. HIGHWAY ONE NORTH / PRINCETON, NEW JERSEY 08540*

## Foreward

The following final report NASA CR-159528, summarizes the technical effort conducted under Contract NAS3-21354 by Princeton Combustion Research Laboratories, Inc. from 18 April 1978 thru 20 December 1978. The Contract was administered by the National Aeronautics and Space Administration, Lewis Research Center, Cleveland, Ohio.

NASA/LeRC Technical Monitor - Thomas H. Cochran

Table of Contents

## Summary

A study was conducted to assess the feasibility of conducting experiments in space on smoldering combustion, to conceptually design specific smoldering experiments to be conducted in the Shuttle/Spacelab System and to provide design information for identified experiment critical components. The analytical and experimental basis for conducting research on smoldering phenomena in space has been established. Physical descriptions of the various competing processes pertaining to smoldering combustion have been identified. The need for space research has been defined based on limitations of existing knowledge and limitations of ground-based reduced-gravity experimental facilities.

The ability of Spacelab to provide a reduced-gravity environment, from a fraction of $g_0$ to zero-g, allows for the possibility of performing a more complete experimental diagnostic investigation of the physical factors involved in the smoldering combustion process. In Spacelab, by taking advantage of the zero-gravity environment, we may observe smoldering in the absence of any free convection, i.e., both forced convection and pure diffusion can be investigated, and by mounting the smolder experiment on a rotating assembly, thus providing an easily varied artificial gravity, it is possible to modify in a systematic manner the free convection component of the internal energy transport.

A further justification for performing smolder combustion experiments in Spacelab is that zero-g and fractional-$g_0$ environments can be provided in order to investigate the nature of the quenching process and, therefore, the limits of smoldering combustion. The importance of improving our understanding of quenching limits is a practical safety matter. This suggests that this would be one of the high priority goals in performing smolder experiments in Spacelab.

List of Figures

# 1. Scientific Justification

## 1.1 Literature Survey

An extensive literature search was conducted during the period of performance of this contract utilizing the facilities of the Princeton University library, NTIS literature survey searches, and the personal collection of Dr. Martin Summerfield based on the extensive experimental and theoretical investigations performed at his Princeton University laboratory on smoldering combustion.

We have assessed this collection of technical literature to identify the derivations and correlations that treat gravity effects and to identify the various competing processes in the governing mechanisms of smoldering combustion. This assessment forms the basis for the scientific justification of the proposed study.

Incorporated in this Contractor Report as Appendix A is the list of relevant references.

## 1.2 Basic Considerations of Smoldering Experiments in a Controlled Reduced-g and Zero-g Environment

Smoldering is a special mode of combustion of a solid fuel that can occur if the fuel body is porous and permeable. Figure 1 presents a tabulation of those areas where smoldering occurs in practice. From a practical standpoint there is a need to understand the mechanism of smolder combustion wave propagation. Smoldering combustion can be driven by forced flow of air, the cigarette being a common example. The smoldering process in cigarette smoking is directly responsible for the formation of carcinogens in the smoke; carcinogens are formed in the smolder reaction zone and are not present as precursors in the tobacco or the paper of the cigarette. Smoldering combustion can also be driven by the natural convection of air, the extensive peat bog fires that surrounded Moscow in the early 1970's being perhaps the most spectacular example. These smoldering peat bogs resisted all common means to extinguish them and the skies remained smokey for most of the year. It may also be possible for a smoldering combustion process to propagate and persist in the absence of any convection (forced or free) at all, that is, by diffusive flow alone, although this has not been observed on earth and cannot be observed in the presence of gravity.

Smoldering combustion is receiving considerable scientific attention at present. One reason is that smoldering driven by natural convection is considered a major fire hazard, particularly due to the widespread use of porous foam rubber materials. Plastic foams, particularly polyurethane foams, are used extensively in modern life. Flexible polyurethane foams are used as mattresses, as seat cushions in automobiles, airplanes, etc.,

1. FIRE HAZARD IN CUSHIONED FURNITURE:

   -INSIDIOUS KIND OF FIRE, CANNOT BE SEEN.
   -POISONOUS GASES EMITTED, WORSE THAN FULL FLAME.
   -MANY DEATHS OF UNSUSPECTING EXPOSED PERSONS.
   -KNOWN FIRE RETARDANTS FREQUENTLY WORSEN SITUATION.
   -NATIONAL BUREAU OF STANDARDS PROGRAM ESTABLISHED.

2. FIRE HAZARD IN PEAT BOGS IN FORESTS:

   -DIFFICULT TO EXTINGUISH, A PERFECTLY SHIELDED "FIRE".
   -MAY LEAD TO FULL FOREST FIRE.

3. FIRE HAZARD IN LARGE COAL PILES.

4. FIRE HAZARD IN INSULATION IN BUILDINGS, RAILROAD CARS, AIRCRAFT CABINS, ETC.:

   -SPECIAL CASE OF CONFINED SMOLDER.
   -PRODUCTS RESEARCH COMMITTEE SPONSORED PROGRAMS TO STUDY SMOLDERING COMBUSTION IN PLASTIC FOAMS.

5. SMOKING OF CIGARETTES, CIGARS, PIPES:

   -FIRST SMOLDER STUDY CONDUCTED AT PRINCETON UNIVERSITY -
   PHILIP MORRIS, INC.
   NATIONAL CANCER INSTITUTE.
   - OBJECTIVE IS REDUCTION OF HEALTH HAZARD, PART OF NATIONAL PROGRAM TITLED, "TOWARD A LESS HARMFUL CIGARETTE".

6. GRAIN ELEVATOR EXPLOSION HAZARD

   -ACCUMULATIONS OF GRAIN DUST, SMOLDERING AT LOW IGNITION TEMPERATURES, MAY INITIATE FIRES OR EXPLOSIONS.
   -SIMILAR INDUSTRIAL HAZARDS IN SUGAR, DRY MILK, LUMBER, ETC., OPERATIONS. (CONCERN OF OSHA, NIOSH, ETC.)

Figure 1. Areas where smoldering occurs in practice.

and as upholstery in most furniture. The manufacture of polyurethane foam rubber is a large industry in the U.S. Rigid polyurethane foams, applied most economically with spray nozzles, are used for thermal insulation in buildings, and for sound and vibration insulation in vehicles such as railroad cars, aircraft, etc. The national push to improve the insulation of buildings for energy conservation is certain to augment such use. These foams, flexible or rigid, constitute a serious fire hazard. They can easily begin to smolder, even if heated to moderate temperatures (600 to 800 K) that would not start a visible flame, and such smoldering combustion is not easily extinguished by conventional fire fighting techniques. Even more disappointing is that the usual fire retardants (for example, TRIS) added to the foams by the manufacturer do not inhibit smoldering, indeed they usually seem to aggravate the smolder danger even though they act to reduce the tendency to open flaming.

The plastic foam industry, specifically twenty-five manufacturers of polyurethane foam and the basic ingredients, was ordered by the Federal Trade Commission in 1974 to take vigorous steps to solve the problem, that is, to reduce the danger of smoldering combustion in such foams. The industry is busy at this task, not only within its own laboratories but also via sponsored research projects administered by a special Products Research Committee set up by the Society for Plastics Industries (SPI).

Generally speaking, a smolder combustion wave propagates through the combustible fuel just as an open flame would propagate, despite the large difference in maximum temperature, ca. 700-1300 K versus ca. 1800 K or more for an open flame, and the large difference in combustion velocity. That is, the factors that determine the speed of propagation of the wave and the peak temperature are, as in all flames:

(1) the chemical kinetics of the reaction, (2) the heat release per unit mass, i.e., the thermochemistry of the reaction, and (3) the transport processes that govern the transfer of energy from the burned region of the combustion wave to the still unburned region.

Smolder combustion propagates much more slowly than a flame and at a much lower temperature because all three of the above factors conspire to slow down the process. In smoldering, the transport of oxygen is usually too slow to support an open flame because of the low permeability of the porous materials involved. The heat release per unit mass of solid fuel is usually low because the stoichiometry of the oxidation reaction may be far from the normal range, in some cases as low as 1% of the air flow required for complete oxidation. The chemical kinetic rates are slow as a result of the low temperatures involved. Although smoldering combustion is essentially a chemical process, the rate of smoldering and the factors that determine the limits of smoldering are dependent in large part on the internal transport processes within the combustion wave.

The main purpose, therefore, of taking smolder experiments into a zero-gravity Spacelab is to permit the experimenter to make controlled variations in the internal transport of energy. The transport processes that are probably the most important in smoldering are: (1) convection of heat by

movement of burned product gases through the fuel body, (2) conduction of heat through the heterogeneous solid-gas structure, and (3) internal radiation of thermal energy from pore-to-pore. Conduction of heat can drive the smolder wave, in principle, in the absence of convection, but heat conduction (and mass diffusion) is always swamped by convection in a ground-based experiment. In a ground-based laboratory, we can do little to affect any of the transport processes without making a basic change in the material or of the confinement conditions, which would simultaneously affect other physical and chemical factors, thus complicating the interpretation of the experimental data. In the Spacelab, however, by taking advantage of the zero-gravity environment, we may observe smoldering in the absence of any convection, forced or natural, and by mounting the smolder experiment on a rotating rig, thus providing an easily varied artificial gravity, it is possible to modify in a systematic manner the natural convective component of the internal heat transport. Interpretation of the data to deduce the transport terms should become less ambiguous, with the convective term varying from zero upward, at the decision of the experimenter.

As explained above, the energy transport rate within the medium determines not only the smolder velocity but also the smoldering limits. One of the most valuable aspects of the Spacelab experiment will be the unraveling of the connection between rate of energy transport and smoldering limits. It has been generally assumed that the inability of some substances to smolder after being ignited is due to certain conditions being outside the limits, and it is assumed that heat loss from the body during start-up of smolder is the cause of going beyond the postulated limits. Unfortunately, there is no quantitative information at all on which to build a theory of limits or of smolder quenching, despite the importance from a fire safety standpoint of understanding just what might prevent smoldering. Very little research has been done in ground-based experiments on the factors that control smolder limits, mainly because of the difficulties in making clear-cut changes that might affect the limits, without affecting other factors. However, by conducting the smolder experiment at successively lower values of gravity (lower rotational speeds) the transport process can be affected without making other changes. This is the main scientific justification for doing smolder experiments in a space-based laboratory, in a reduced-g environment.

Various ground-based laboratory experiments on smoldering combustion have been performed by Dr. Summerfield and associates (Ref. 33,34 and 48) with flexible, open-cell polyurethane foams, granulated cellulosic materials, granulated polyisocyanurates, and phenol formaldehyde rigid foams. These experiments included free and forced convection in both the counter-current and co-current modes. Schematic representations of the temperature, $O_2$ concentration, and fuel concentration distributions for forced convection are shown in Figure 2. It is interesting to note the following qualitative features of smoldering combustion. The smolder wave thickness is larger for the counter-current mode in granular cellulosics than that of the co-current mode for flexible polyurethane foams. All the available fuel is consumed in counter-current smoldering of granulated cellulosics while the residue remaining from co-current smolder of flexible polyurethane foams is fuel-like in character. The fuel concentration of the residue represents only a small percentage decrease from the original foam

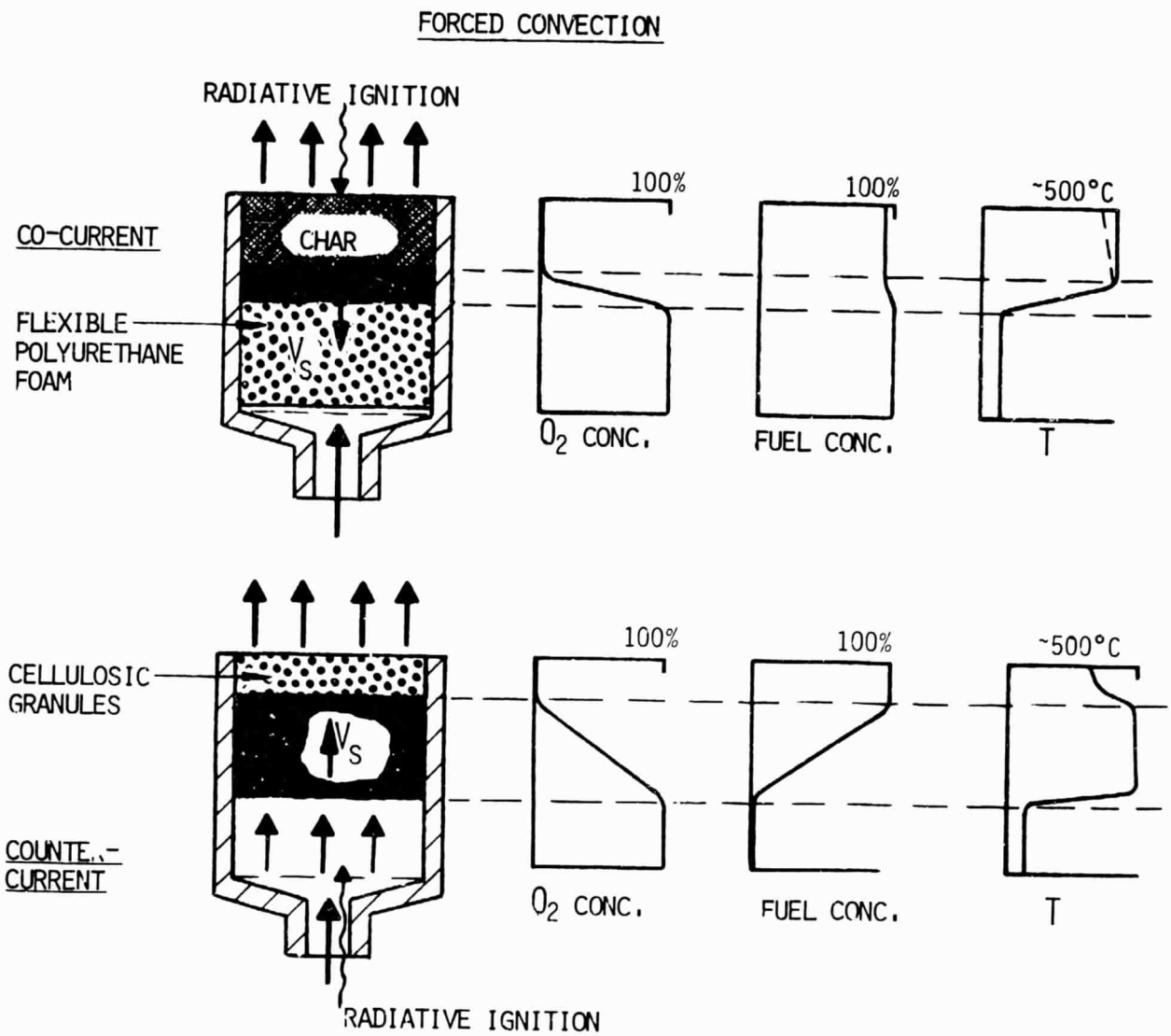


Figure 2. Schematic Representation of Temperature, $O_2$ Concentration, and Fuel Concentration Distributions for Forced Convection Smolder Combustion.

fuel. The smoldering combustion process is oxygen starved. That is, all available oxygen is utilized, at least in those cases where the oxidizing environment is air. The peak temperature associated with smoldering combustion is considerably less than the adiabatic flame temperature. Of course, quantitative results are a function of gas upflow rate in the controlled forced convection experiments.

The preceding discussion can be made clearer by considering in a quantitative manner the processes occurring in a natural-convection smolder wave. To fix the ideas, we consider a cannister containing a porous, permeable, combustible body of fuel (e.g., polyurethane having a density of about 1/20 $g/cm^3$) in the form of a solid cylinder with impermeable side-walls, as shown in Figure 3.

The longitudinal profiles of mass flux and temperature in the two media, solid and gas, as seen in a frame of reference moving with the combustion wave, are pictured qualitatively in the following graphs:

CO-CURRENT CASE

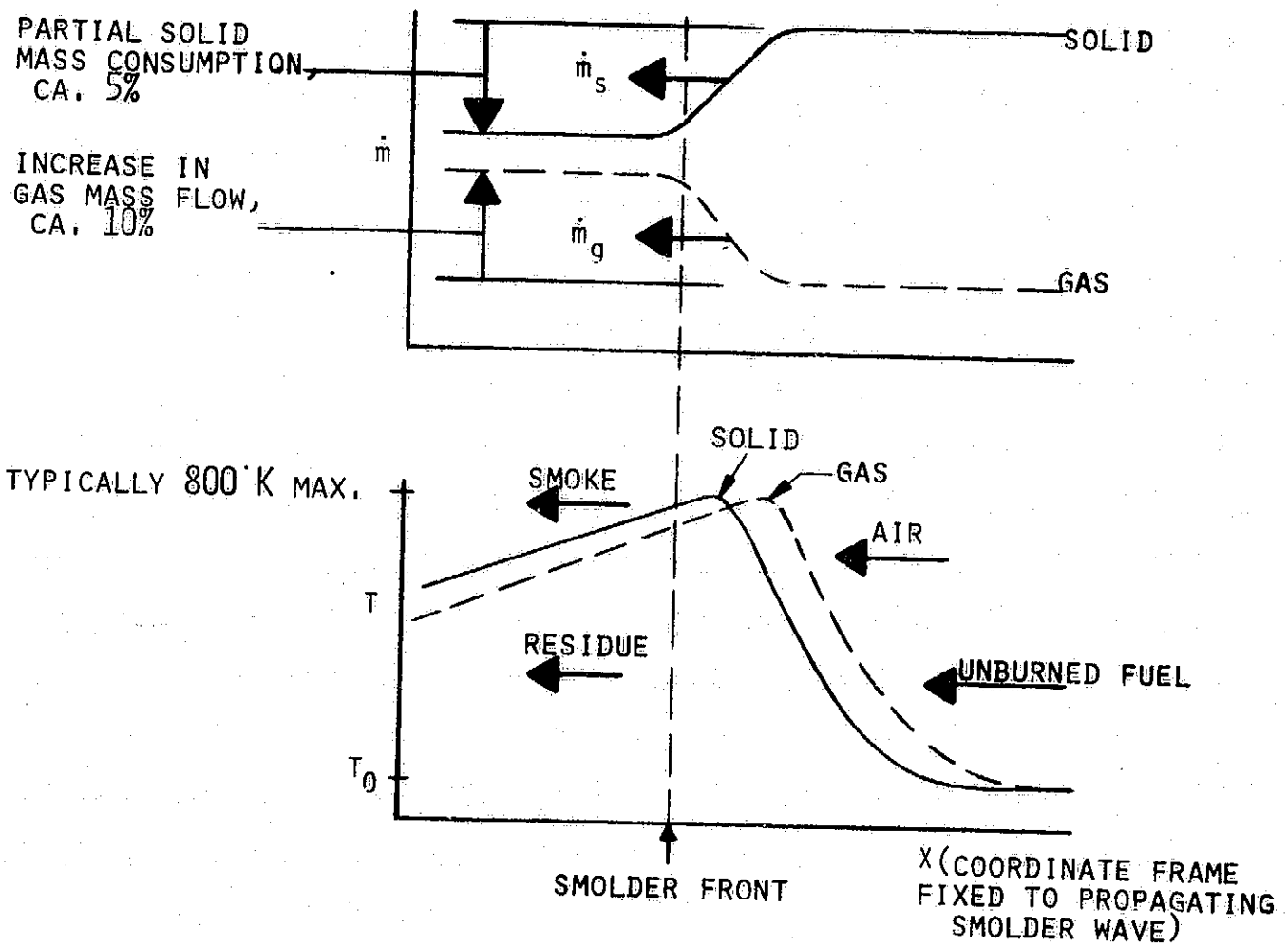

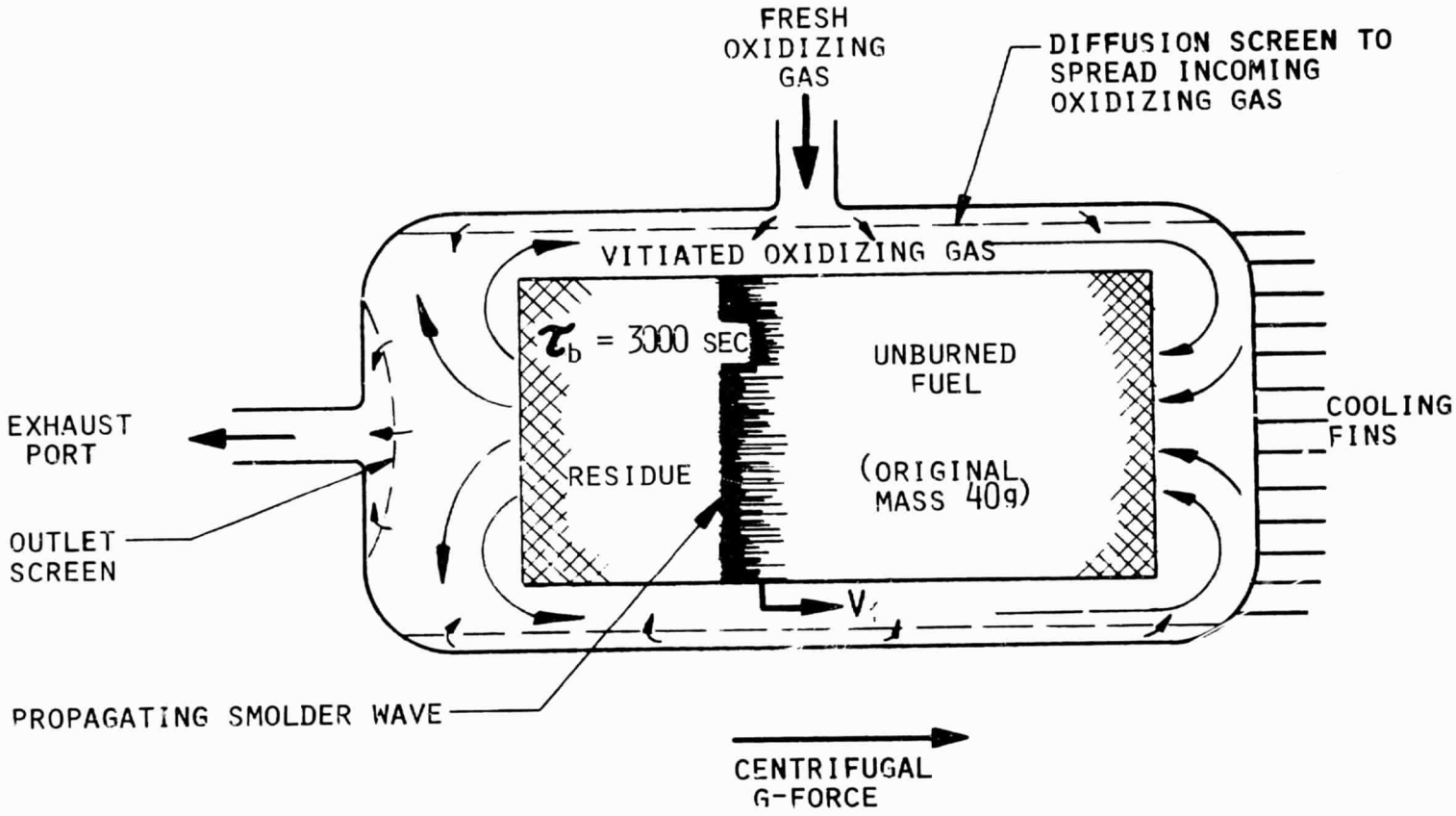


Figure 3. Schematic Representation of Smolder Cannister Housing Combustion Fuel: the Co-Current Case.

The assumptions underlying this physical picture are the following:

1. The combustion wave moves with a constant velocity through the solid medium, the induced air flow rate is also constant with time, and the distributions shown above remain constant with time. (This is the most severe approximation employed in the present discussion; it is not necessarily valid for the experiments proposed for Spacelab.)

2. The temperature of the solid is very close to that of the gas stream at all stations along the wave. That is, although there is indeed a difference of temperature between the two media, associated with the different heat transport processes, the difference is small and can be ignored in an analysis of this kind, as long as the essential energy equation is satisfied. (The alternative would be to write <u>two</u> energy equations, one for the solid, the other for the gas, and an equation for the heat exchange rate between the two media. This additional complication is eliminated by recognizing that the two temperatures are virtually the same at every point.)

3. The inter-diffusion of species in the longitudinal direction is neglected. In general, in flame theory, such neglect introduces some error in the theoretically predicted flame speed, but the physical picture remains essentially unaltered. For the purpose of this brief review, we have ignored this complication. For the case of smolder at zero-g, when natural convective transport goes to zero, the diffusion terms become very important, of course. We recommend that the analysis with inclusion of the diffusion terms in the energy equation, as well as the species conservation equations, be carried forward early in the effort of placing the smoldering combustion experiment onboard Spacelab. It is not known a priori at what level of reduced-g the diffusion terms might overtake the convection terms.

4. Simplifying assumptions such as neglecting the temperature dependence of air viscosity and air density, neglecting the change in permeability of the solid as it degrades and burns, etc., will not materially alter the essential conclusions.

With these assumptions in mind, the one-dimensional propagation problem can be analyzed by means of the governing equations of continuity, momentum and energy. For the purpose of explaining the physical processes involved, the approximate magnitudes of the important terms will be developed here, also.

The <u>mass continuity equation</u> in integrated form (steady state), referred to the moving frame of reference, can be written simply as follows (with typical values shown below each term):

$$\dot{m}_s \qquad \pm \qquad \dot{m}_g \qquad = \qquad \text{Constant}$$

$$2 \times 10^{-4} \text{ g/cm}^2 \text{ sec} \qquad\qquad 1 \times 10^{-4} \text{ g/cm}^2 \text{ sec}$$

In the differential form, the continuity equation is:

$$\frac{\dot{dm}_s}{dx} = \pm\frac{\dot{dm}_g}{dx} = \pm w_s \quad \begin{array}{l}\text{(rate of gasification of solid/unit volume)} \\ \text{(Order of magnitude, } 10^{-6} \text{ g/cm}^3 \text{ sec)}\end{array}$$

The sign convention used is that mass flow to the right is positive, to the left, negative.

From a chemical reaction standpoint, the mass changes involved in the continuity equation can be represented by:

$$\overbrace{C_{1.0}H_{1.78}N_{0.07}O_{0.32}}^{\text{FOAM}} + \overbrace{0.061(O_2 + 3.72N_2)}^{\text{AIR}} \rightarrow \overbrace{0.94(C_{1.0}H_{0.85}N_{0.13}O_{0.12})}^{\text{CHAR}}$$

$$+ \overbrace{0.034CO + 0.031CO_2 + 0.26H_2 + 0.23H_2O + 0.20N_2}^{\text{PRODUCT GAS}}$$

Unfortunately, as explained in the section on stoichiometry, present knowledge of the composition of the product char and of the product gases is somewhat incomplete, even in the case of polyurethanes, which have been investigated more than other porous substances. Thus, the presence of hydrogen in the large amount shown above, needed to balance the equation after the measured concentrations of CO and $CO_2$ and the measured composition of the char are taken into account, is open to doubt. Other organic gases, generated possible in the pyrolysis zone, in the particular co-current smoldering experiments that served as a basis for the above stoichiometric analysis, might perhaps be considered in the balancing of the equation, such as acetaldehyde or ketones, but no definite information is available on this point. Analytical measurements will have to be made prior to the Spacelab experiments.

Numerical values typical of smoldering (taken from experiments with polyurethane foam in a co-current mode) are the following:

Loss of mass from foam to char, less than 10%
Average rate of foam gasification across the whole smolder wave, about $10^{-6}$ g/sec per $cm^3$
Heat release in smoldering, as a fraction of complete heat of combustion to $CO_2$ and $H_2O$, about 5 - 10%
Stoichiometry: only about 5% of stoichiometric air is reacted
Stoichiometric ratio for complete combustion, 8.8 g air/1.0 g foam by weight
Mass flow rates (in moving frame of reference), typically 2.0 foam/1.0 air
Heat of combustion of residual char, about 85 - 90% of that of foam
Heat of combustion of product gases, about 10% of that of foam although there is uncertainty as to product gas composition
Increase in gas volume flow rate, from entering air to product gas, nearly 200% (which includes uncondensed water vapor), more

than a third of it being hydrogen from the pyrolysis zone preceding the oxidation zone of the smolder wave. (But see reservations about this in the Stoichiometry Section.)

The diagram shown previously for the two mass flows versus distance X illustrates the rate of change of mass flow as a consequence of the chemical kinetics of the reaction, which involves both pyrolysis and oxidation. The approximate values placed in the diagram indicate that only about 5% of the solid is consumed in the co-current smoldering reaction, in the polyurethane experiments previously mentioned. (Higher percentages may be encountered at higher g-levels, in other materials, and perhaps in counter-current smoldering instead of co-current smoldering.) Since the typical smolder wave is supported by a mass flow of air that is only one half of the mass flow of solid, i.e., far from the stoichiometric ratio of 8.8 required for complete combustion, the 5% loss of mass flow of solid in the diagram is reflected in a gain of 10% in mass flow of air going through the wave.

The momentum equation (steady-state) for the air flow running through the porous solid, expressed in the same moving frame of reference, is:

$$\frac{dp}{dx} + \frac{d(\dot{m}_g u_g)}{dx} = -(f_B \mu_g) u_g - \rho_g g$$

The first term on the right side is the viscous drag term, i.e., resistance law, associated with the finite permeability of the solid. This term is taken as proportional to the first power of the mean velocity, i.e., Poiseuille flow. This is justified by the very low Reynolds Number of the porous flow, about $10^{-2}$ based on pore diameter. Departure from the linear law toward the square law begins to be significant in porous media above a Reynolds Number of about 10. The resistance coefficient is dependent, of course, on porosity and on pore-connectedness. The coefficient of proportionality (about 10 micro-atm per cm/sec air velocity based on observed buoyant air flow rates in laboratory experiments), is shown as divided into two components, one, the viscosity of the air, the other, the resistance coefficient. In taking them here as constants, we are admittedly glossing over the fact that the viscosity varies strongly with local temperature in the smolder wave and the fact that the resistance coefficient varies as the pore structure degrades during pyrolysis and oxidation of the porous body. In future analysis, these variations will have to be taken into account.

The acceleration term on the left side turns out to be negligible in comparison with the other terms in the equation, and so it can be dropped. This is true not only in the burned and unburned sides of the wave but inside the reaction wave (where the air density change is most rapid) and at the end-faces of the porous body as well, where the air velocity changes rapidly. With the assumptions of constant air properties, constant resistance coefficient, etc., the remaining terms can be integrated to provide the momentum equation in integrated form:

$$(p_1 - p_2) = (f_B \mu_g) \bar{u}_g L + \bar{\rho}_g \bar{g} L = \bar{\rho}_a \bar{g} L$$

This is of interest because it introduces the so-called buoyancy "force" that drives the hot air and combustion products. The right-hand member of the double equation is the gravitational weight of the cool air surrounding the porous test cylinder, which determines the pressure difference between top and bottom expressed by the left-hand member above. This right-hand member is the "constant of integration" of the differential equation.

Re-arranging the terms, we get an equation that shows the role of buoyancy:

$$\bar{u}_g = \frac{(\bar{\rho}_a - \bar{\rho}_g)\cdot\bar{g}}{(f_B \mu_g)} = \frac{\text{buoyancy force}}{\text{resistance}} \approx \frac{1 \frac{\text{micro-atm}}{\text{cm}}}{10 \frac{\text{micro-atm}}{\text{cm}^2/\text{sec}}}$$

It should be noted that, in writing the momentum equation in differential form above without any buoyancy term, it corresponds to the fact that the cylindrical porous body is sealed on the sides, that air cannot enter or leave the cylindrical surface, and that the external isobars of the surrounding "atmosphere" cannot penetrate directly into the combustion domain. However, the pressure difference of the external atmosphere <u>does</u> make itself felt as a <u>boundary condition</u> on the integrated momentum equation. In this way, the density difference that we commonly call buoyancy makes its appearance in the final equation, as shown above. This feature was chosen for the design of the experiment in order to assure a nearly one-dimensional flow field. Had the cylindrical surface been permeable, the buoyancy term would have appeared right in the differential equation, but the one-dimensional flow picture would then be incorrect.

The <u>energy equation</u> can be written as follows:

co-current case

$$\dot{m}_s c_s \frac{dT}{dx} \pm \dot{m}_g c_g \frac{dT}{dx} = q_{comb} + \lambda_{cond} \frac{d^2T}{dx^2} + \frac{dq}{dx}_{rad} - q_{loss}$$

counter-current case

| | | | | | | |
|---|---|---|---|---|---|---|
| 0.063 | 0.021 | 0.063 | 0.021 | 0.021 | 0.021 | $(J/cm^3 sec)$ |
| (0.015) | (0.005) | (0.015) | (0.005) | (0.005) | (0.005) | $(cal/cm^3 sec)$ |

where, $\dot{m}_s$ = mass flow rate of solid per unit area, in frame of reference fixed to propagating smolder wave

$c_s$ = specific heat of solid

$\dot{m}_g$ = mass flow rate of oxidizing gas per unit area, in frame of reference fixed to propagating smolder wave

$c_g$ = specific heat of oxidizing gas, at constant pressure

$q_{comb}$ = combustion heat release rate per unit volume

$\lambda_{cond}$ = thermal conductivity of porous body

$q_{loss}$ = heat loss rate per unit volume

$q_{rad}$ = net of leftward minus rightward pore-to-pore radiation/unit area internal to the porous body in the axial direction.

The sign in front of the term associated with the air flow depends on whether the combustion wave proceeds in the same direction as the air flow (negative, like a cigarette being smoked) or in the opposite direction (positive, like a foam cushion smoldering as a result of ignition by a cigarette dropped on its surface). In the planned experiments, under natural convection conditions, this term can be made to go either way, the plus sign by igniting the porous medium on the "upper" surface so as to generate a co-current combustion wave, the minus sign by igniting the porous body on the "bottom" surface so as to generate a counter-current combustion wave. With forced convection under zero gravity conditions (no natural convection), the plus or minus sign can be made to go either way by choice of the surface to be ignited or by choice of the direction of forced air flow.

Our purpose here being merely to display the magnitudes of the important physical terms, not to derive a theoretical solution for the temperature distribution or the wave velocity, we have used the measured characteristics of a typical smolder wave in polyurethane cushion foam under co-current natural convection as a set of inputs to derive the numbers shown below each term:

Peak temperature, ca. 800K (ca. 500C)

Flame width, ca. 5 cm

Flame velocity, $5 \times 10^{-3}$ cm/sec relative to the solid

Induced air flow velocity (at sea level gravity), 0.1 cm/sec

Heat of combustion of the porous material (to $CO_2$ & $H_2O$), $3 \times 10^4$ kJ/kg (7500 cal/g)

Heat of combustion of the porous material in smoldering, $1 \times 10^3$ kJ/kg (250 cal/g)

Completeness of combustion (corresponding to $1 \times 10^3$ kJ/kg), 3.3%

Density of the porous medium, 0.05 g/cm$^3$

Fraction of void volume, 95%

Resistance of porous body to air flow during smoldering (linear velocity range), 10 micro-atm per cm per cm/sec air velocity

Specific heat of solid, 1.2 kJ/kg K (0.3 cal/g C) (average)

Specific heat of the air, 1.0 kJ/kg K (0.25 cal/g C) (average)

Average pore size (enters into estimate of internal radiative heat transfer from pore to pore) ca. 0.02 cm (200 microns)

Thermal conductivity of porous body (with pores filled with air at 800 K (ca. 500 C), $1.2 \times 10^{-1}$ W/m$^\circ$K ($3 \times 10^{-4}$ cal/sec cm C)

A separate theoretical computation of the internal transport of heat by radiative exchange from pore-to-pore yields the following formula for the heat-up term in the energy equation:

$$\frac{dq_{rad}}{dx} = 4\varepsilon\sigma\delta\left[3T^2\left(\frac{dT}{dx}\right)^2 + T^3\left(\frac{d^2T}{dx^2}\right)\right] \approx 12\varepsilon\sigma\delta\, T^2\left(\frac{dT}{dx}\right)^2$$

at "rise" of wave

where $q_{rad}$ = net of forward and reverse pore-to-pore radiation internal to the porous body in the axial direction, leftward being positive

$\varepsilon$ = emissivity of the solid surface of each pore

$\sigma$ = black-body Stefan-Boltzmann constant

$\delta$ = pore size (effective radiation path length)

The pore size is used as the effective radiation path length in the internal exchange process, on the assumption that the air is transparent and the solid is not. The thermal emissivity of the solid is taken as unity for the low temperature infra-red radiation occuring in the smolder wave.

The above-listed thermal conductivity of the porous solid (95% void) filled with air at ca. 800 K was calculated by means of a simple mixing rule for two substances, air and solid, the former having a thermal conductivity of $1.2 \times 10^{-1}$ W/m°K ($3 \times 10^{-4}$ cal/sec cm C) and the latter having a value of 0.4 W/m°K ($1 \times 10^{-3}$ cal/sec cm C). The air volume being the greater by 20:1, its higher resistance dominates the mixed conductivity.

The chemical kinetic rate of heat release within a co-current smolder wave is estimated from the observed overall rate of heat release to be about 4 kJ/kg (1 cal/g) of solid per sec at the peak of the wave. On a unit volume basis, averaged through the smolder wave, the heat release rate is about 0.06 J/cm$^3$ sec (0.015 cal/cm$^3$ sec). This would be consistent with the observed thickness of the reaction zone and the low density of the porous solid. At this slow rate, it takes about 10-15 minutes for the solid at a particular point in the wave to go through the entire chemical reaction.

Making use of the physical values listed above, one can compute approximately the values of the several terms in the steady-state energy equation. They are given underneath the respective terms of the energy equation, above. Of course, these are merely approximate or average values; the terms vary from point to point in the wave, as the temperature and char condition vary along the wave. Also, it is evident that there is some guesswork in obtaining the needed physical and chemical kinetic values. Nevertheless, several significant conclusions are possible.

One is that it is indeed possible for so very slow an oxidation reaction as that involved in co-current smoldering to provide the rate of heat release required to sustain a smolder wave. That is, the heat release rate is enough to bring the energy equation into balance; it is commensurate in value with the other terms in the equation. This might not have seemed so

self-evident at first, when it is noted that the combustion efficiency in co-current smoldering is only a few percent (in some cases as low as 1%), that the heat release is only about 1 x $10^3$kJ/kg (250 cal/g) of solid, and that the leftover char has an atomic composition that indicates that it is almost as good a fuel as the original unsmoldered fuel. The char left over is still capable of releasing as much as twenty times the heat that was released in the oxidation process in the smolder wave. In fact, under proper experimental conditions, the char can be re-ignited to smolder again, e.g., a porous body that has smoldered completely in the co-current mode can support a counter-current wave. This raises a relevant question: If the leftover char is still a good fuel, why is it not consumed more completely in the first combustion process?

We suspect that the resolution of this question may involve the same factors that determine smolder limits or quenching, in this case operating within the combustion wave after it has passed over the porous fuel and after the fuel has partially burned. If, as has been suggested, the kinetic rate of heat release, already quite feeble, is slowed further at the tail end of the passing smolder wave by the thermal degradation of the polymer and the carbonizing of the surfaces of the pores, making the heat production term too weak to overcome the heat loss term, then the reaction would stop after a certain stage is reached. This suggests that smolder limits might be found at low gravity levels (low rotational speeds in our proposed apparatus) in materials that smolder readily at normal gravity levels. Reduction of gravity would reduce the air flow, slowing the reaction. Similar smolder limits (quenching limits) may be found at low oxygen concentrations, which can also slow down the oxidation reaction, and at reduced air pressure, too. In fact, it is possible that we will find a four-fold theoretical connection between (1) the quenching that terminates the oxidation of the fuel as the smolder wave passes over it, (2) the quenching at low oxygen concentrations, (3) the quenching at reduced air pressure, and (4) the quenching at low gravity levels in a Spacelab experiment. The importance of improving our understanding of quenching limits of smoldering -- a practical safety matter -- suggests that this would be one of the high priority goals in performing smolder experiments in a Spacelab.

The way to gain such improved understanding, of the smolder process more generally and not simply of the quenching process, is to perform experiments that reveal the magnitudes of the several terms in the energy equation and how they vary with different conditions. In the proposed Spacelab experiments, it will be possible to vary at will the effective gravity and hence the induced air velocity. By means of imbedded thermocouples in the solid, the profile of the temperature wave can be determined, and also the wave velocity can be measured. By means of the oxygen concentration sensors, the oxygen usage can be measured, and if the cannisters can be recovered for chemical analysis of the char left after the passage of the smolder wave, the thermochemistry can be worked out. (Some assumptions will have to be made, of course,to make up for incomplete analysis, in that it is not planned to measure all the effluent gases in situ.) The net result will be that the respective terms of the energy equation can be evaluated, at least approximately, for each test. It will then be possible, for example, to observe how the terms vary as the

quenching limit is approached. We believe this will clarify the mechanism of quenching. More generally, it will be possible to observe how the respective terms vary with different conditions and it may be possible to deduce "laws" for such variations. This may permit the evolution of a general theory of smoldering, something that is not possible at this time because such "laws" are not known. (We speak of laws here in the same sense that a chemical engineer might speak of the chemical kinetics of a reactor or a gas turbine combustor; the laws are semi-empirical, not truly fundamental in nature, but the entire literature of combustion systems rests on such laws, sometimes called global kinetics.)

It should be noted also that it was merely for convenience of the discussion that the preceding conservation equations for the smolder process were written in steady-state form without time derivatives. In treating the temperature profiles and other measurements to be obtained from Spacelab experiments, the full equations with time-dependent variables, i.e., with time derivatives, should be employed to interpret the data. It is doubtful that, in so short a distance of travel of the smolder wave, the planned 15 cm, it would reach a true steady-state; moreover, there are reasons to believe that, at least in the counter-current mode, a steady-state may not be possible.

Admittedly, this kind of diagnostic investigation of the smolder process and of the structure of the smolder wave can also be attempted in ground-based laboratory experiments. However, since systematic variation of the induced air flow is not readily feasible at a fixed gravity, the limitations of choice of the remaining parameters do not encourage the belief that useful generalizations can be deduced from such experiments; and so in the past such experiments have not been pursued.

It would indeed be useful to perform experiments with varying gravity at levels above 1 $g_0$ by running a spinning apparatus of the kind proposed herein in a ground-based laboratory. This has not been done in the past, and there are no plans that we know about to so such experiments. It would be a good idea to include a program of this kind as a ground-based study prior to placing the experiment in the Spacelab. It should be recognized, however, that performing experiments on smoldering at gravity levels above 1 $g_0$ will not substitute for the proposed experiments at reduced gravity (down to zero). The quenching phenomenon that we have discussed above will be encountered, we believe, most readily by going to weak gravity, for any substance that smolders easily at normal gravity.

Thought has been given to the possibility of performing the desired diagnostic experiments in a forced flow smolder experiment (such forced flow experiments have been performed before in the laboratory), but the presence of gravity in a ground-based experiment means that we cannot be confident that the flow velocity at each point in the fuel body is just that corresponding to the imposed flow rate. Gravity induced flows at 1 $g_0$ are just as strong as the forced convection flow, when the latter is regulated down to the level corresponding to realistic smoldering, and so severe distortion in local velocities due to gravity may be expected in ground-based forced flow experiments. Interpretations from such tests, e.g., magnitudes of the terms in the energy equation and deducing the desired "laws", will be open to challenge. However, we do

recommend in the experimental plan for the Spacelab that forced flow experiments be performed as part of the test matrix; these would be done only at zero gravity, that is, at zero spin velocity.

Thought has been given also to the possibility of conducting a smolder experiment at zero gravity (zero spin) with no forced flow, that is, with only diffusion operating to transport the air (or oxygen) and heat. The mass diffusion differential equation was not presented above; the approximation was made that only convection was operative. It is difficult to estimate the diffusive velocity in a porous medium, but in a free space the diffusive velocity of oxygen within a reaction zone several centimeters thick would be much less that the 0.1 cm/sec quoted above. We suspect that, in a porous matrix, the effective velocity will be still less, too slow to overcome quenching. Still, it should be tried. It can be done with the same cannisters designed for forced convection tests and reduced-g free convection tests.

It should be noted also that, useful as such forced flow experiments will be for diagnostics of the smolder wave (when performed at zero gravity), they may reveal nothing about the nature of quenching under natural convection tests. Smoldering with natural convection is basically a coupled process: the heat release is governed by air flow rate, and the air flow rate is governed by the heat release rate. In such coupled processes, the breakdown of the process -- quenching in this case -- may be the result of something more subtle, perhaps a dynamic instability rather than a static failure. Therefore, forced flow tests, being basically uncoupled smolder situations, may not reveal at all the proper quenching limits or the mechanism of quenching. For this reason, we intend to be alert to differences between the quenching limits as they may be found in the natural convection varying-gravity smolder experiments and the limits as they may be encountered in the forced-flow zero gravity experiments.

In conclusion, the justification for performing smolder experiments in the Spacelab rests on two main premises, first, that with the ability to provide variable gravity all the way down to zero it will be possible to perform more complete experimental diagnostic investigations of the factors involved in the smoldering process and thus improve our theoretical understanding of smoldering combustion, and second, that the extra parameter that varying gravity makes available will improve our theoretical understanding of the nature of the quenching process, that is, of the limits of smoldering combustion.

## 1.3 Mechanisms of Smolder

Smoldering combustion is a mode of non-flaming burning which differs from normal combustion in several ways. Usually the combustible medium is porous in structure, permitting air to flow into the smolder reaction wave to support the driving heterogeneous oxidation process. Smoldering is characterized by extensive thermal degradation of the virgin material, evolution of smoke, incomplete combustion, and little or no emission of visible light. The temperature of smolder is always much less than the

flame temperature of the same fuel when burning in the normal open-flame mode with air. The propagation velocity is usually much less than normal mass burning rates in open flames. The term smoldering is usually applied to situations in which natural convection is sufficient to drive the needed air into the reaction zone, thus sustaining the combustion process, but forced-flow smoldering is quite possible, too, e.g., a cigarette during the puff. Not all combustible substances will support smoldering combustion: some will not react with sufficient exothermicity under the lean air-flow conditions (only a few percent of stoichiometric air) to support a propagating wave. Some materials will not provide the correct degree of balance within the smolder wave between the heat evolution process and the heat dissipation process, both of which are directly related to the natural convection process. In some cases, unfavorable geometry or low permeability may inhibit the smolder process, leading to a non-self-sustaining process and extinction.

The smolder phenomenon is exhibited in a wide variety of organic materials, including carbon, coal, various woods and wood products, tobacco, other cellulosic materials, dusts, and synthetic polymers, including such foams as polyurethanes, polyisocyanurates and phenol formaldehyde. Extensive experimental studies on the smoldering aspects of polymer foams and cigarettes have been performed by Summerfield, et al. (32,34 and 48), the results of which form the basis for the following description of the physical mechanisms controlling the smolder phenomenon.

Flexible polyurethane foams exhibit a broad spectrum of smoldering behavior dependent upon various parameters: mode of ignition, $O_2/N_2$ ratio of the surrounding environment, forced air flow rates (including the limiting case of zero forced air flow, the free convection limit), co-current or counter-current flow situation, foam permeability and cell structure, and heat loss mechanisms. The following scheme can be postulated for foam degradation, represented schematically in Figure 4.

Any mathematical formulation of the physical mechanism of smolder must account for the various degradation pathways observed in TGA/DSC experiments. If a smolder wave is established in the material it will either be self-sustaining, i.e., a heat feedback mechanism to the smolder front is sufficient to drive the smolder wave in a propagating fashion, or it will be non-self-sustaining, i.e., extinguishment will ensue. Also, depending on the oxidizing environment, that is, the $O_2/N_2$ ratio and pressure of the oxidizing gas, and depending on the air flow rate, transition to flaming may result. Another alternate degradation pathway is the formation of a melt (tar) that impedes the propagation of the smolder wave by destruction of the open cellular structure.

It is postulated that, for a self-sustaining smolder wave to exist, the virgin foam when heated by the ignition source partially oxidizes exothermally. However, it can be shown in TGA experiments that the oxidation is ordinarily preceded by endothermic degradation. The degraded foam further decomposes in the presence of an oxidizing environment to yield a char layer and volatiles. In ground-based experiments a continuous supply of oxidizing gas is ensured by the fact that the gases within the open cell structure are subjected to an upward buoyancy force (natural convection)

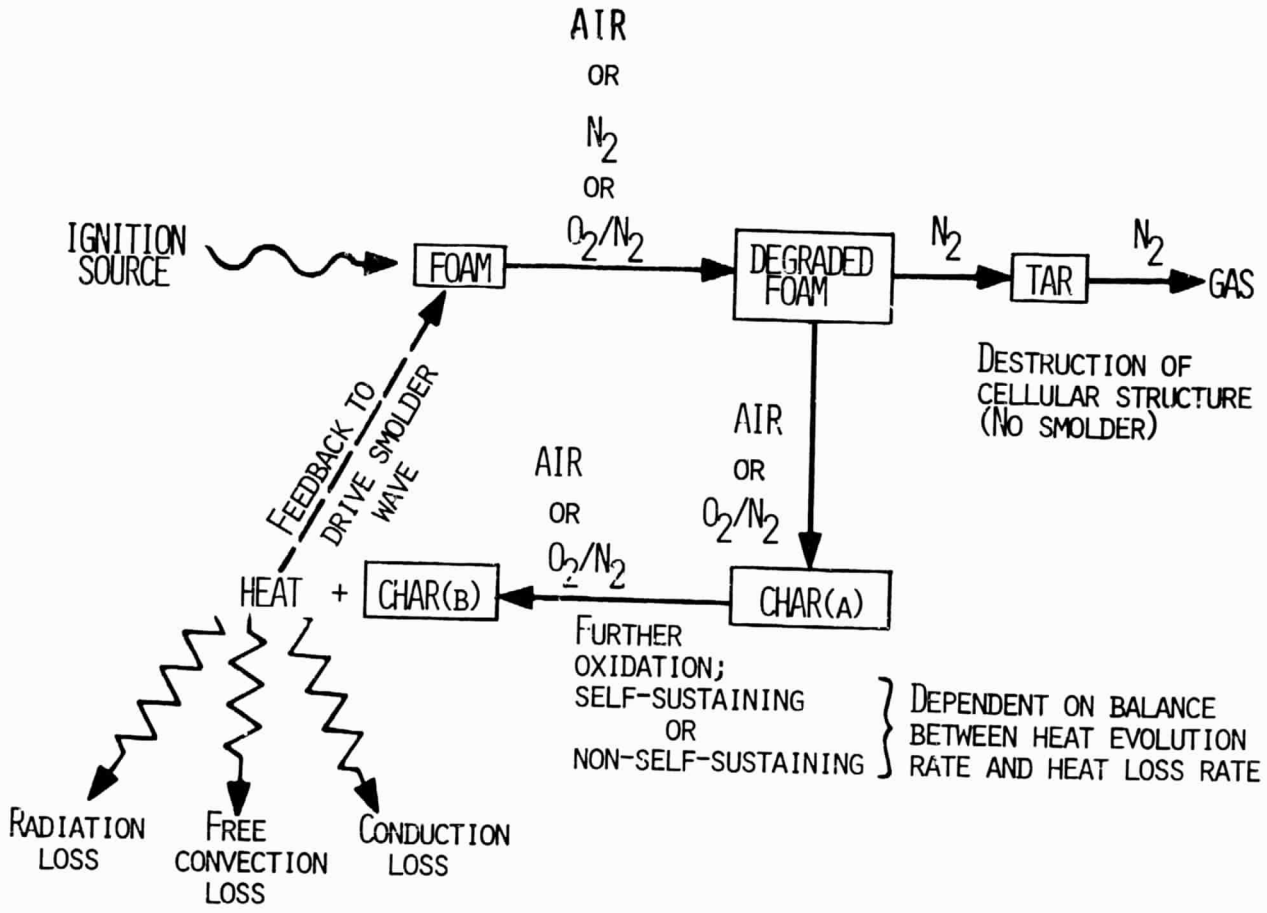


Figure 4. Degradation Pathways of Polyurethane Foam in Smoldering Combustion.

when they are heated. The key here is the open cell structure. It has been observed in the case of polyurethane smolder that the cellular structure of the char layer is similar to that of the virgin foam. The maintenance of the original open cell structure permits the convection of oxygen into the burning zone and the char layer for further oxidation. The oxidative attack on the char liberates heat. It is this char oxidation process that is the heat source for the developing smolder process. If the heat liberated by the char oxidation process fed to the smolder reaction front is sufficient to overcome local heat sinks, e.g., radiation loss, free convection loss, and conduction loss, the smolder wave is sustained and propagates further into the virgin foam.

## 1.4 Stoichiometry

### 1.4.1 Complete Combustion of Polyurethane Foam in Air

The stoichiometric equivalence ratio for complete combustion of Firestone foam H2528 is readily computed from its elemental analysis: $C_1H_{1.78}N_{0.07}O_{0.32}$*. Consider the following stoichiometry:

$$\overbrace{C_1H_{1.78}N_{0.07}O_{0.32}}^{\text{FOAM}} + X\ \overbrace{(O_2 + 3.719\ N_2)}^{\text{AIR}} \longrightarrow r\ CO_2 + s\ H_2O + t\ N_2$$

where it is assumed that $H_2O$ is in the vapor state.

The atomic balance equations are:

C: $r = 1$

H: $2s = 1.78$; $s = 0.89$

N: $0.07 + 7.438\ X = 2t$

O: $0.32 + 2\ X = 2r + s$

*The elemental compositions of foams and char are taken from Reference 48.

Solving these equations for the unknowns r,s,t and X:

$r = 1$
$s = 0.89$
$t = 4.814$
$X = 1.285$ (= O/F ratio)

Next, we compute the heat release for complete combustion to $CO_2$ and $H_2O$. It has been estimated that,

$$\Delta H^{O}_{f_{foam}} = 34 \text{ kJ/formula weight (8.0 kcal/formula weight)}$$

From standard thermochemical tables,

$$\Delta H^{O}_{f_{CO_2}} = -394 \text{ kJ/mole (-94.1 kcal/mole)}$$

$$\Delta H^{O}_{f_{H_2O}} = -242 \text{ kJ/mole (-57.8 kcal/mole) (if water vapor is not condensed)}$$

Then, the heat liberated by the above combustion reaction is

$$-Q_c = \sum_i (n_i \Delta H^{O}_{f_i})_{\text{products}} - \sum_i (n_i \Delta H^{O}_{f_i})_{\text{reactants}}$$

or

$$Q_c = 643 \text{ kJ (153.5 kcal)/ formula weight of foam reactant}$$

or

$$Q_c = 32 \text{ kJ/g (7.7 kcal/g) of foam reactant}$$

That is, 32 kJ (7.7 kcal) of heat are liberated per gram of foam for complete combustion of the foam. This corresponds to 8.8g of air required to fully burn one gram of this polyurethane material.

### 1.4.2 Actual Products of Smolder Combustion in Air

Based on ground-based co-current experiments performed with flexible open-cell polyurethanes, it is observed that the solid products of smolder combustion are a char-like residue comprised of a complex C,H,O,N material whose final composition is quite sensitive to the smolder conditions. The fraction of virgin foam converted to this char residue is a function of both heating rate and oxygen availability. The chemical nature of this residue varies considerably over the range of conditions. The only chemical examination of the char residue from the Princeton University program has been an elemental analysis of a sample consumed by natural convection co-current smolder. The result was:

$$C_1H_{0.85}N_{0.13}O_{0.12}$$

This is compared to the elemental analysis of the virgin foam:

$$C_1H_{1.78}N_{0.07}O_{0.32}$$

Thus we see that H and O are depleted relative to the C of the original foam, but N is increased. (The latter is difficult to explain, except that the amount is small and subject to error.)

The variability of gaseous products of smolder combustion is indicated in Figure 5, extracted from Reference 48. Product gases were withdrawn from forced convection experiments performed in a Buchner funnel (see Figure 6) with a forced gas upflow rate of 0.15 cm/sec (of the same order as one-$g_o$ natural convection flow velocities). Sampling was limited to the product gases CO, $CO_2$ and $O_2$ as the percentage of $O_2$ in the flowing gas was varied.

Several points are worth noting:

(i) All the available $O_2$ is consumed in the smolder process, except for oxygenated air in which the $O_2/N_2$ ratio exceeds 40%/60% by volume, indicating that the smolder process is oxygen starved and limited by oxygen availability.

(ii) As the percent of $O_2$ is increased, an increase in the oxidized product gases CO and $CO_2$ occurs, commensurate with the higher observed peak temperature of the smolder wave. Since the experiments were performed at $O_2/N_2$ ratios not in the vicinity of the flaming limit, it is anticipated that the percentage of CO must peak and then decline to zero as the flaming limit is approached.

These experimental results provide a means of estimating the heat release per gram of foam during the smolder process. Consider the following stoichiometry:

$$C_{1.0}H_{1.78}N_{0.07}O_{0.32} + X(O_2 + a\ N_2 + b\ CO_2) \longrightarrow$$

$$Y\ (C_{1.0}H_{0.85}N_{0.13}O_{0.12}) + x\ CO + y\ CO_2 + z\ H_2O + p\ H_2 + q\ N_2 + r\ O_2$$

We include $H_2O$ (vapor) in the above equation since it may be present but cannot be extracted from the product gases ($H_2O$ vapor would tend to condense). We assume that r = 0, that is, we confine our attention to those cases where all the available oxygen is consumed.

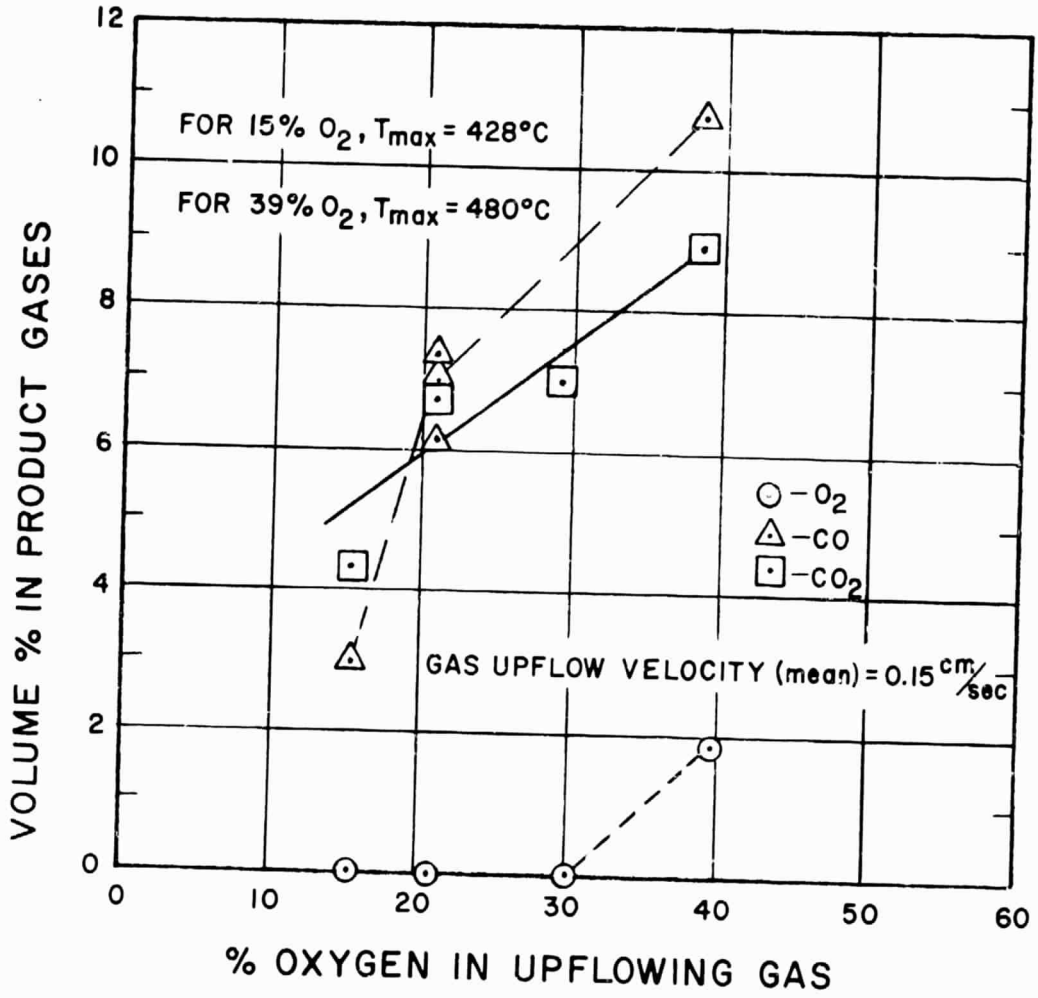


Note: a) Complete consumption of $O_2$ (below 30-40% $O_2$).

b) Sharp increase in carbon monoxide even as $O_2$ availability increases.

Figure 5. Effect of Oxygen Availability of Selected Smolder Product Gases.

(Flexible, open-cell polyurethane foam; co-current mode. Taken from Ref.48)

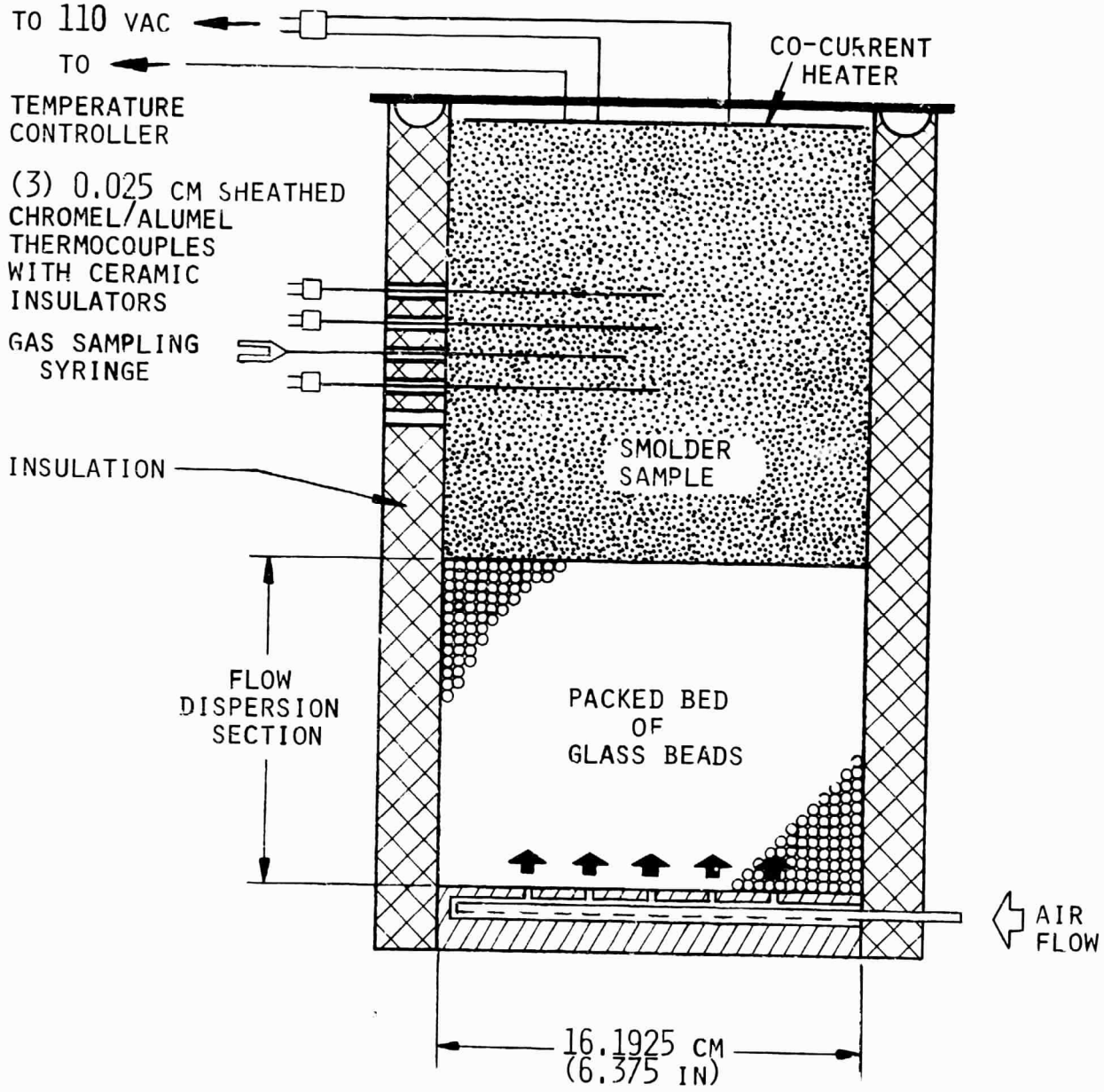


Figure 6. Cross-Section of Buchner Funnel Smolder Apparatus Utilized in Princeton University Co-Current Smolder Experiments.

The unknowns to be determined are : X,a,b,Y,x,y,z,p,q (nine unknowns). The atomic balance equations for C,H,N,O provide four of the nine equations required to determine the nine unknowns. These four balance equations are:

C: $1 + bX = Y + x + y$

H: $1.78 = 0.85\ Y + 2\ z + 2\ p$

O: $0.32 + 2\ X + 2\ b\ X = 0.12\ Y + x + 2\ Y + z$

N: $0.07 + 2\ a\ X = 0.13\ Y + 2\ q$

Additionally, the experimental data in Figure 5 provides the following two relationships:

$x/(x + y + p + q)$ = % CO in product gas

and

$y/(x + y + p + q)$ = % $CO_2$ in product gas

where it is assumed that $H_2O$ has condensed before reaching the gas chromatograph.

This provides 6 of the required 9 equations.
Also if we define:

$V_f$ = velocity of the smolder wave relative to the solid

$V_a$ = oxidizing gas velocity through the porous material

$\rho_f$ = apparent density of porous material (fuel)

$\rho_a$ = density of oxidizing gas

$\dot{m}_f$ = mass flow rate of porous material (fuel) in a frame of reference fixed to the propagating smolder wave

$\dot{m}_a$ = mass flow rate of oxidizing gas in frame of reference fixed to propagating smolder wave

$N_f$ = moles of fuel

$N_a$ = moles of oxidizing gas

$MW_f$ = molecular weight of fuel

$MW_a$ = molecular weight of oxidizing gas

$X = N_a/N_f$

We have,

$$\frac{V_f \rho_f}{V_a \rho_a} = \frac{\dot{m}_f}{\dot{m}_a} = \frac{N_f MW_f}{N_a MW_a} = \frac{MW_f}{X\ MW_a}$$

where $V_f$ is observed experimentally for a given $V_a$, $\rho_f$, and $\rho_a$

and

$$MW_a = \text{MW of } (O_2 + a\ N_2 + b\ CO_2)$$

$$MW_f = \text{MW of } (C_{1.0}H_{1.78}N_{0.07}O_{0.32})$$

Rearranging the above equation:

$$X = \left(\frac{MW_f}{MW_a}\right)\left(\frac{V_a \rho_a}{V_f \rho_f}\right).$$ This is the seventh observable that can be used in the system of analysis for the nine (9) unknowns. Two more relationships are required to form a determinate set of equations. These are provided by the conditions under which the smolder experiment was performed, that is, the known weight percent of $O_2$, $N_2$, and $CO_2$ in the upflowing oxidizing gas. Hence, a and b are known.

Consider the case in which the volume percentage of oxidizing gas constituents is $O_2/N_2$ = 0.21/0.78. This corresponds to a weight percentage at STP of $O_2/N_2$ = 0.232/0.755 and $CO_2$ percent (b) equal to zero. On a molar basis, considering 100 g of fuel, this corresponds to 0.725 mole $O_2$ and 2.696 mole $N_2$, or, normalizing by the number of moles of $O_2$, we have

$$a = 3.719$$

$$b = 0$$

For oxidizing gas containing 21%/78% volume percent of $O_2/N_2$ the results of Figure 5 indicate that the volume percentages of CO and $CO_2$ in the product gases are, respectively, 6.50% and 5.85%.

For a smolder wave propagation velocity of $1.2 \times 10^{-2}$ cm/sec and oxidizer gas upflow rate of 0.15 cm/sec, as determined from Figure 7.

$$V_f = 1.2 \times 10^{-2} \text{ cm/sec}$$

$$V_a = 0.162 \text{ cm/sec}$$

The apparent density of Firestone Polyurethane Foam No. H2528 is $4.01 \times 10^{-2}$ g/cm$^3$ (= $\rho_f$). The density of the oxidizing gas mixture is $1.23 \times 10^{-3}$ g/cm$^3$ (= $\rho_a$) at STP.

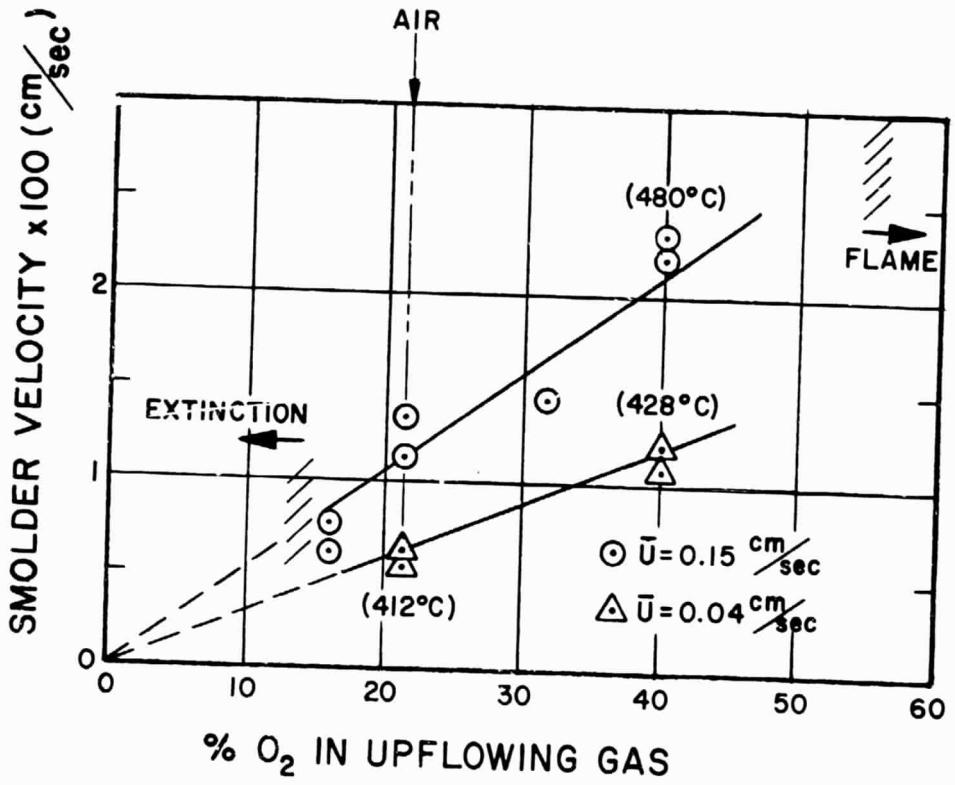


Figure 7. Effect of Oxygen Upflow Rate on Smolder Velocity.

(Flexible, open-cell polyurethane foam; co-current mode. Taken from Ref.48).

Also,

$$MW_a = MW_{O_2} + a\, MW_{N_2} = 136.13$$

$$MW_f = MW_C + MW_{H_{1.78}} + MW_{N_{0.07}} + MW_{O_{0.32}} = 19.88$$

Therefore,

$$X = 0.0605 \quad (= O/F \text{ ratio})$$

Solving the previous set of equations, we obtain

$$Y = 0.935$$
$$x = 0.034$$
$$y = 0.031$$
$$z = 0.233$$
$$p = 0.262$$
$$q = 0.200$$

If we compare the oxidizer/fuel ratio for this case to the oxidizer/fuel ratio for complete combustion of the polyurethane foam, we find that the equivalence ratio for smoldering combustion is 4.7% of stoichiometric air (complete combustion). This would imply a heat release of 1510 J/g (360 cal/g) of foam for smoldering combustion for the case of 0.15 cm/sec upward oxidizing gas flow velocity and $O_2/N_2$ ratio of 21%/78% by volume. This number appears to be compatible with observed low peak temperatures in the smolder wave.

However, if the heat release is computed from the heats of formation of the various molecules indicated in the balance equation for smoldering combustion, i.e.,

$$Q_c = \sum_i (n_i \Delta H^o_{f_i})_{\text{products}} - \sum_i (n_i \Delta H^o_{f_i})_{\text{reactants}}$$

we find that $Q_c$ = 3600 J/g (860 cal/g) of foam. This is based on the assmuption that the heat of formation of both the virgin foam and char material is zero. This implies that the heat release is approximately 11% of that obtained for complete combustion of the polyurethane foam, rather than 4.7%. In either case, of course, 0.41 g of air are utilized in smoldering combustion of one gram of polyurethane foam.

The discrepancy noted above in the heat liberated during the smoldering combustion process is cause for concern. Several factors may contribute to this inconsistency:

(i) The elemental analysis of the char material was performed on a specimen which had undergone smoldering combustion under natural convection conditions rather than the forced flow conditions in which product gas composition was analyzed. A small change in the conditions of the experiment, i.e., oxidizing gas flow rate, can affect

the composition of the char which, in turn, critically affects the stoichiometry and resulting heat release. It has recently come to our attention that three independent tests of the composition of the char material resulted in the number of gram-atoms of hydrogen per gram-atom of carbon being as low as 0.55 and as high as 0.90.

(ii) The literature reveals that acetaldehyde is a likely candidate for the product gas composition, rather than $H_2$. The fact that the above computations indicate a significant percent of $H_2$ in the product gas, far in excess of CO, is a clue that we must pursue the question of stoichiometry further. The product gas $H_2$ was never sampled in the experiments.

Note that our initial conjecture that the volumetric gas produc ion from smoldering combustion is on the order of 10% of inflowing oxidizing gas volumetric flow may have been much too conservative. The above computation indicates that this contribution may be more accurately represented as a 200% increase. It all depends on whether $H_2$ is indeed as prominent in the exhaust gas as indicated above.

All of this uncertainty suggests that, as part of the planned Spacelab experiment, stoichiometry and thermochemistry are subjects that deserve study in the overall smoldering combustion project.

## 2. Conceptual Design of Experiments

This phase of the study included the following:

1. Definition of Spacelab conditions and constraints relevant to the planning of the smoldering combustion experiments, as derived from NASA sources of information. These include physical constraints, time constraints, operational constraints, etc.

2. Conceptual experiment configuration designs. Two different cannister configurations are considered as candidates for the Spacelab experiments in order to achieve the desired objectives of the smoldering combustion studies. The factors considered in the design of the individual smoldering combustion cannisters were: choice of size and shape, annular clearance required for natural convection pumping action of oxidizing gas, flow rate of oxidizing gas needed to support smoldering combustion and to scavenge away combustion products, orientation of cannisters, etc.

3. Definition of matrix of test variables: Selective identification of primary test variables and test matrix to adhere to time constraints as discussed previously, so as to achieve the desired objectives of the smoldering combustion experiments.

4. Choice of smolder materials.

5. Identification of sub-systems to be considered in the total experiment design. The various sub-systems identified are:

   (i) Rotating support structure
   (ii) Individual smolder cannisters
   (iii) Driving motors and shaft assemblies
   (iv) Motor speed control system
   (v) Electric power sources/requirements
   (vi) Oxidizing gas flow rate controls
   (vii) Oxidizing gas supply system
   (viii) Combustion gas exhaust system
   (ix) Smolder combustion instrumentation
   (x) Data acquisition and recording system
   (xi) Ignition system
   (xii) Safety assurance system
   (xiii) Pre-launch check-out system

## 2.1 Definitions of Spacelab Conditions and Constraints

The preliminary design of the Combustion Facility proposed by NASA Lewis Research Center and documented in NASA Applications Notice Spacelab 3 presents constraints on the design of the smoldering combustion test apparatus. Physical constraints such as Combustion Facility chamber dimensions and service port size and number limit the overall dimensions of the apparatus. The Combustion Facility chamber as presently conceived by NASA is a cylinder 0.61 m (24 inch) in diameter and 1.5 m (59 inch) in height. The preliminary design of the smoldering combustion experiment, discussed in Section 2.2 below, must accommodate sufficient smolder cannisters so that the desired test matrix can be conducted within 4-5 hours. This time constraint must also allow for installation time, preliminary check-out time, experiment time and disassembly time. We believe that the design discussed in Section 2.2 below, in conjunction with the test matrix planned, will achieve the desired results within the time constraints.

The access ports of the presently conceived Combustion Facility chamber present constraints with regards to assembly of the smoldering combustion experimental apparatus. According to recent documentation, NASA has designed the Combustion Facility chamber with three elliptical access ports, 0.25 m (10 inch) by 0.15 m (6 inch), major and minor axes, respectively. Two are oriented vertically, one near the top and one at the middle of the chamber. The third is oriented horizontally and located near the bottom of the chamber. This arrangement makes assembly of a large fixture difficult. The positioning of the access ports is not as convenient as a common glove box. While the experimental design presented in Section 2.2 has taken this into account, the assembly remains cumbersome and time consuming. It is our recommendation, therefore, that a re-design of the access ports be considered in favor of a hatch (door) entrance. The weight of such a hatch entrance to withstand the pressure differential allowable by NASA between Combustion Facility chamber and Spacelab environment ($\pm 10.3$ N cm$^{-2}$, i.e., 1.0 atm), should not be excessive. Another alternative to save the time of the astronaut-scientist is to assemble the proposed smoldering combustion experiment within the Combustion Facility chamber prior to launch. Thus, only the disassembly time becomes nonproductive time within the 4-5 hour time constraint. Figure 9, presented in the discussion of Section 2.2, clearly displays the relationship between the experimental apparatus and the Combustion Facility chamber.

It has been stated by NASA that the allowable short term adiabatic heat release to the Combustion Facility chamber is approximately $9.81 \times 10^4$ J (100 BTU), based on only external air cooling of the combustion chamber walls. The heat release in the smolder process of Firestone Polyurethane Foam No. H2528 is considerably less than that associated with the stoichiometric value (ca. $31.4 \times 10^3$ J/g foam or $7.5 \times 10^3$ cal/g foam), which can be seen to be compatible with the low peak temperatures of the smolder process. At low gas velocities through the smolder material the indicated equivalence ratio is ca. 3% of stoichiometric, indicating a heat release per gram of foam of ca. 1050 J/g (250 cal/g) of foam. Since each cannister contains 30 g foam material (based on considerations presented in Section 2.2 and assuming that all material in the cannister is to be consumed, this implies

$31.4 \times 10^3$ J ($7.5 \times 10^3$ cal) heat release per cannister. The present test plan strategy calls for smoldering combustion experiments to be performed in 8 cannisters at the same time, yielding a total heat release of $2.5 \times 10^5$ J ($6.0 \times 10^4$ cal or 255 BTU). It should be realized, however, that this is a long-term adiabatic heat release estimate, based on the smolder process requiring approximately 50 minutes at 1 g equivalent to consume the entire sample in the co-current mode (smolder wave velocity approximately $0.5 \times 10^{-2}$ cm/sec). The long-term smolder heat release may lie well within the limits of acceptability depending on clarification of the term "short-term" adiabatic heat release and depending on the degree of adiabaticity of the cannister exhaust process over a 50 minute duration.

It should be realized for smolder combustion in the counter-current mode, a ten-fold decrease in sample consumption time may result, assuming that the degradation pattern favors char formation rather than tar (or melt) formation. Again, the degree of adiabaticity of the cannister exhaust process over a short term, possibly 5 minutes, needs investigation.

In order to reduce the heat release associated with the smolder combustion process in each cannister we can relax the requirement that the smolder wave propogate through the entire porous fuel body. Extinguishment of the smolder combustion process by depletion of the oxidizing gas environment, i.e., shut-off of oxidizing gas supply, and initiation of a $N_2$ purge has been incorporated into the design as a safety measure anyway and can be adopted for this purpose. Alternatively, the Combustion Facility chamber can be equipped with a cooling system.

Pure oxidizing gas or mixtures of oxidizing gas for the smolder experiment are to be provided by NASA onboard the Spacelab. At present, NASA is considering high pressure storage tanks for $N_2$ and $O_2$ to be metered through an orifice plate to produce user-required mixture ratios of $N_2/O_2$ in a mixing chamber. The pressure of the gaseous mixture is regulated into the Combustion Facility chamber according to user flow requirements. The gas is assumed to equilibrate at ambient temperature prior to entering the chamber. No active gas temperature control is presently planned by NASA.

These constraints on mixture ratio and gas mixture temperature do not present serious problems to the planned smoldering combustion experiments. The test matrix, discussed in Section 2.3 calls for varying the $O_2/N_2$ ratio of the oxidizing gas. This will require the use of separate orifice plates in each feed line from the high pressure $N_2$ and $O_2$ storage tanks to the mixing chamber in order to achieve the desired $O_2/N_2$ ratio in the mixing chamber. The fact that no active gas temperature control is presently planned by NASA is unfortunate, but since the temperature of the oxidizing gas is not planned as a test variable, simple knowledge of the entering gas temperature will have to suffice for the purposes of the experiment and can be obtained via thermocouple measurement in the feed line to the test apparatus. Of course, active temperature control is desirable, since the temperature level of the oxidizing gas can then be preset and maintained. If NASA is not prepared to include an active temperature control in the Combustion Facility, then it is the responsibility of the individual experimenters to incorporate such a design in respective experiment designs if the need arises. It should be

realized that for combustion experiments of long duration, such as the proposed smolder combustion experiments, large excursions of the temperature of the oxidizing gas from the mean equilibrated temperature level, greater than ±10%, cannot be tolerated. This supports the need for an active temperature control.

The space environment can produce a variety of non-gravity associated accelerations that can induce gas and fluid motion. The accelerations in a reduced-g environment which may cause induced convective flows can be grouped into two general categories: those which are steady, uniform weak acceleration fields and those which are temporally-varying and act as perturbations on an otherwise steady reduced-g environment. The magnitudes of these reduced-g accelerations and their influence on induced convective flows must be assessed. Induced convective motions in reduced-g space environments has been a subject of concern in the NASA Materials Processing in Space program, and much of the documentation in Reference 37 is applicable to the NASA Combustion Facility program.

The accelerations causing induced convective motion are:

I. Steady, due to

- (i) atmospheric drag
- (ii) centripetal force due to vehicle rotation
- (iii) gravity gradients
- (iv) solar wind
- (v) solar pressure

II. Temporally-varying accelerations, due to

- (i) engine burns
- (ii) attitude-control maneuvers
- (iii) onboard vibrations from machinery and astronaut movement (voluntary and involuntary)

The magnitude of the steady accelerations, extracted from Reference 37, are:

| | |
|---|---|
| atmospheric drag | $5 \times 10^{-5} g_0$ |
| centripetal force | $1 \times 10^{-6} g_0$ |
| gravity gradient | $3 \times 10^{-9} g_0/cm$ |

As contrasted to the steady accelerations which are part of the natural environment of an orbital vehicle, temporally-varying acceleration perturbations exist which may disturb the local reduced-g field and hence the local convective motion. These time-varying accelerations are referred to as g-jitter and arise from spacecraft maneuvers, mechanical vibrations, and interior movement of personnel. It has been noted (51) that spacecraft maneuvers can produce g-jitter magnitudes of $10^{-2} g_0$. We must assume that it is unlikely that the proposed smolder combustion experiment can take place during the drift mode of Spacelab, since spacecraft maneuvers are likely to occur several times an hour and the duration of a single smolder combustion experiment can be as long as one hour. Therefore, the effect of

the g-jitter associated with engine burns and attitude control maneuvers on the smolder combustion experiment must be considered. Onboard mechanical vibrations that are transmitted to the experiment have the same effect as a temporally-varying reduced-g field. These may be associated with onboard rotating machinery and scientist-astronaut movement during the course of experimentation. During Skylab experiments the g-jitter associated with mechanical vibrations has been estimated to be no larger than $10^{-3} g_0$. It is our opinion that induced motion associated with steady and temporally-varying accelerations will have minimal impact on the smolder experiment.

Another perturbation considered was the Coriolis acceleration associated with the velocity of the combustion gas radially inward in the rotating apparatus. It can be shown that this perturbation never exceeds 1/1000th of the centrifugal g in any of the contemplated operating conditions. It was therefore considered to have a negligible effect on the smolder combustion experiment.

## 2.2 Conceptual Experiment Configuration Design

As stated previously, a prime objective of the Spacelab experimentation on smoldering combustion in porous material is to characterize the structure of the smolder wave in reduced-g environments and to determine the factors that critically affect the tendency toward smolder extinguishment. In the neighborhood of the extinction limit, the smolder process is a fine-tuned balance between the heat dissipation process in the vicinity of the propagating smolder wave and the heat generation rate of the smolder process itself. This, in turn, is critically dependent on the oxidizing gas flow rate through the porous material which drives the smolder process and which is, itself, modified by the heat generation rate.

In order to assess the critical role of the coupling of the buoyancy-driven convective pumping of air and the associated heat release rate from the reaction zone as a function of the magnitude of the effective g-level, particularly in the neighborhood of the extinguishment limit, the following experiment is proposed.

We consider the structure represented schematically in Figure 8. This is a conceptual design of a variable reduced-g smoldering combustion test apparatus. The cannisters, each containing smolder material, associated probing devices, oxidizing gas inflow orifice and exhaust product exit orifice, and ignition source are mounted onto a hollow rotating half-shaft (the shafts above and below the stationary center body are each termed half-shafts) via miniature quick-connects. These quick-connects provide a convenient means of mounting the individual cannisters to the rotating half-shaft and also provide an inlet for the flow of oxidizing gas and provide structural support for the cannister. A given level or tier of cannisters comprises four cannister units. Rotation of the half-shaft and attached cannisters is accomplished by means of a variable speed phase locked loop electric motor. A stationary center body is employed to house shaft bearings, rotating unions for gas lines, and slip rings for signal pick-off. This center body represents a plane of symmetry with two counter-rotating half-shafts to

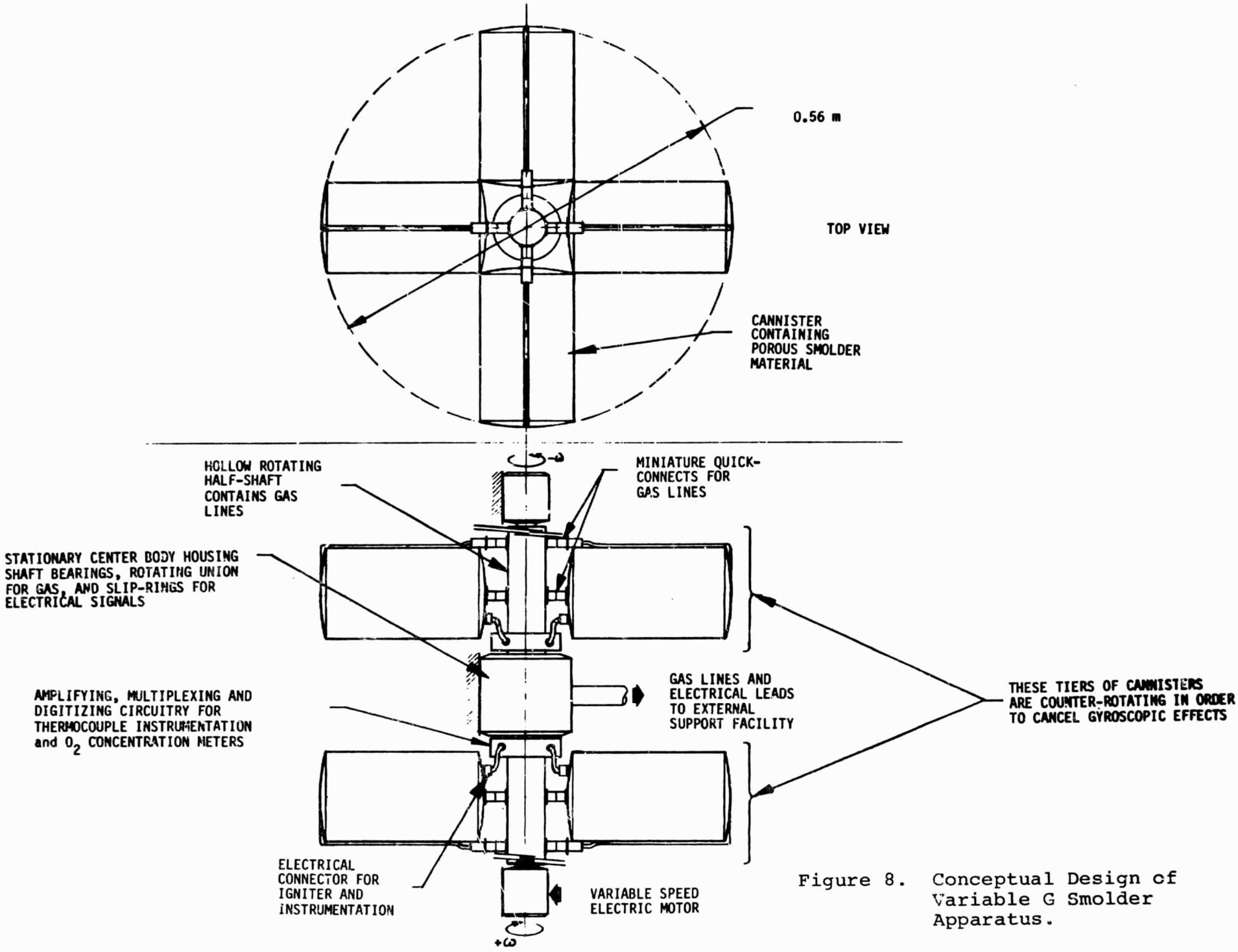


Figure 8. Conceptual Design of Variable G Smolder Apparatus.

cancel gyroscopic effects. The radius of this rotating fixture from shaft centerline to cannister end is 28 cm. The Combustion Facility chamber height of 1.5 m limits the number of levels or tiers of cannisters that can be accommodated on the counter-rotating shafts. Although the conceptual design of Figure 8 depicts only one level of cannisters on each half-shaft, design analysis indicates that four such levels can be accomodated on each half-shaft without interfering with the Combustion Facility chamber internal dimensions. The preliminary design will not present serious problems in terms of assembly or disassembly of the apparatus in the Combustion Facility chamber, although assembly and disassembly will be awkward and time consuming.

A schematic representation of the variable reduced-g smoldering combustion test apparatus within the Combustion Facility chamber is depicted in Figure 9. Also shown are the positions of the service ports relative to the placement of the apparatus.

A total of thirty-two cannisters containing smolder material samples are shown mounted to two motor driven counter-rotating shafts; 16 cannisters per shaft. A Slo-Syn Model M111-FD12 D.C. stepping motor rated at 3.0 J (425 oz-in) torque is mounted at the top and bottom of the Chamber for rotating the shafts. Start-up torque, bearing drag, and gas union seal drag were considered in choosing motor torque. The motors are driven by Slo-Syn Translator Modules type STM 103. The Translator Modules are associated with the stationary electronics. Two hollow shafts (termed half-shafts) 60 cm (24 in) in length, support the cannisters and contain small tubing for supplying oxidizing gas and wiring for data transfer for each cannister. Mounted on the exterior of the shafts is the electronics associated with data conditioning and retrieval. Electrical connections to the cannisters are made via miniature multi-pin connectors. One end of each shaft couples with the motor shaft while the other end is fitted with a three ring slip ring assembly, the inboard ball bearing and rotating gas unions. See Figure 10.

The slip rings carry power, ground and Command & Data transmissions between the stationary electronics and the rotating cannisters. The slip ring assembly would be a specifically designed unit similar to the Electro-Miniatures model AJ-2003 except with a higher current rating to accommodate igniter power requirements. Brush generated noise for this unit is only 100 microvolts maximum.

The inboard ball bearing is a Boston #67069-NR-1640-DS and would be press fit onto the end of the shaft. The D.C. stepping motor bearings act as the outboard bearings for the rotating shafts.

In order to supply oxidizing gas to the rotating cannisters, the inboard ends of the shafts are machined with an alternating series of O-ring grooves and collecting grooves that serve as rotating gas unions. Figure 10 shows this arrangement for supplying oxidizing gas to each of the four tiers of cannisters on one rotating shaft. Small tubes running inside the hollow shafts each connect to a different collecting groove located between two rotating O-ring seals. Incoming gas ports in the stationary center body feed oxidizing gas to the collecting grooves while the shaft is rotating, providing a continuous supply of gas to the rotating tiers of cannisters.

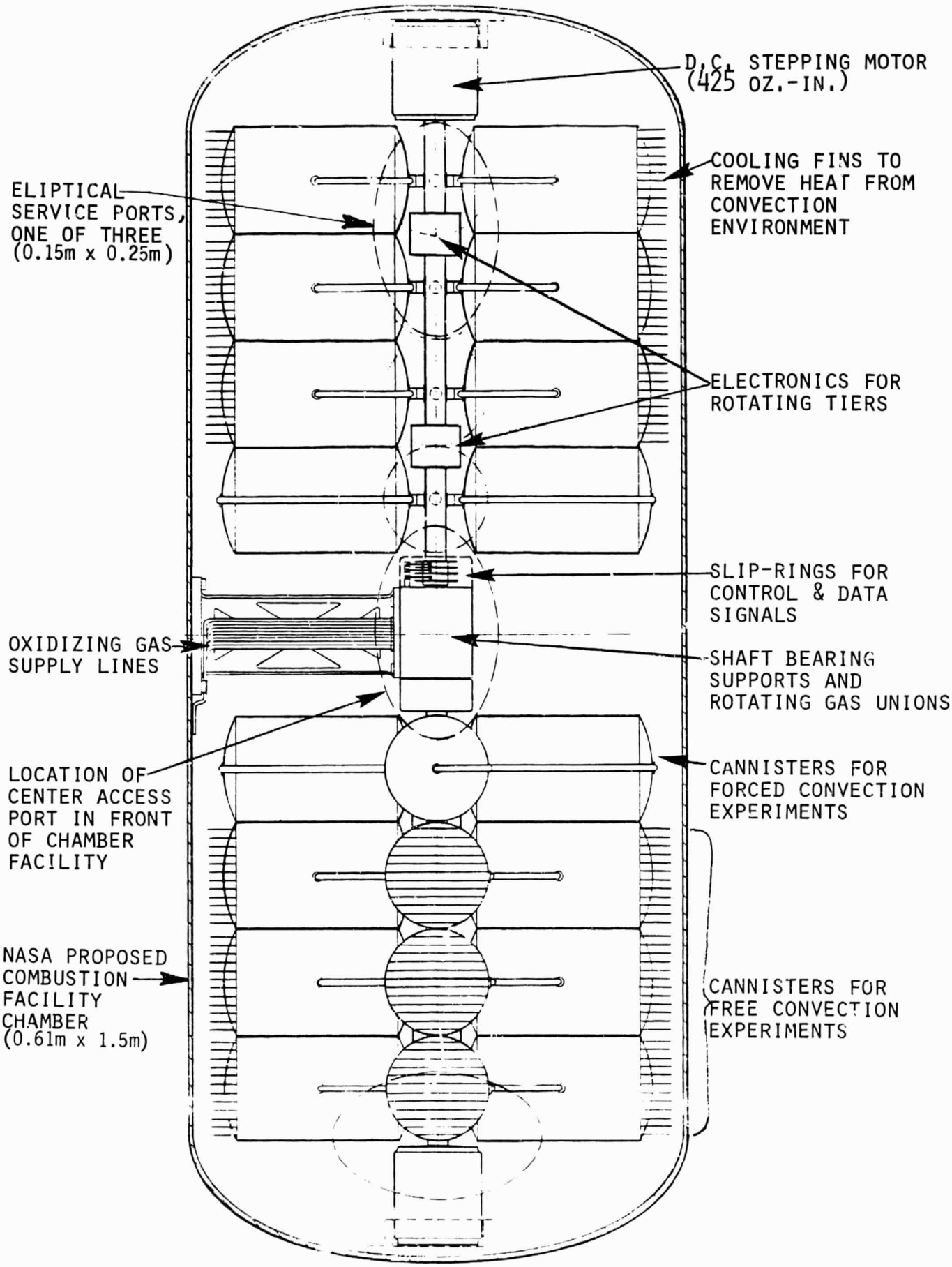


Figure 9. Smolder Experiments Mounted in Combustion Facility Chamber.

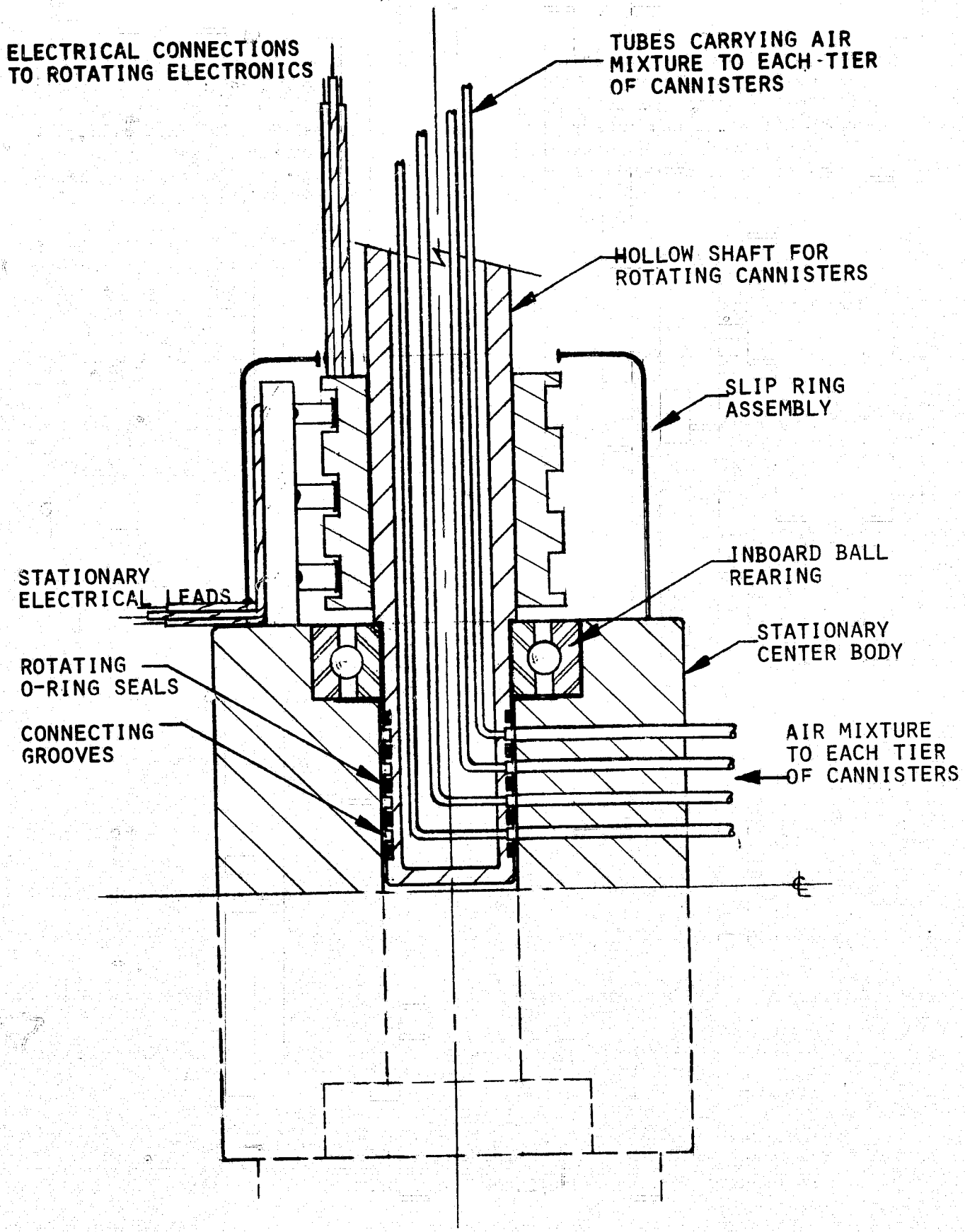


Figure 10. Detail of Rotating Gas Unions, Shaft Bearing, and Slip Rings for One Rotating Shaft.

The cannisters are attached to the shafts via Tomco Model #6020 Mini-Quick-Connects. Located at four circumferential positions equally spaced around the hollow shaft for each tier, these quick-connects serve as mechanical support for the cannisters in the rotating mode as well as inlet oxidizing gas supply for the cannisters. As previously mentioned, electrical connections to the cannisters are accomplished with miniature multi-pin connectors. The cannisters can simply be plugged-in to the shafts in one motion and all electrical connections and gas supply are completed.

Oxidizing gas flow rate will be manually adjusted for a tier of cannisters prior to a test series. Flow rates to individual cannisters will be monitored via Thermo-Systems, Inc. Model #2233 miniature thin film anemometer type mass flow meter. These units, approximately 0.635 cm (0.250 in) in diameter, measure very low flow rates (30 $cm^3$/sec max.) and are temperature compensated.

Two different cannister configurations are under consideration and have been conceptually designed. These are represented in Figures 11 and 12. In all cases the smolder material sample length is 15 cm. The choice of sample length is dictated by the following factors:

(i) Measured self-sustaining smolder wave propagation velocities must be uninfluenced by the presence of the thermal radiation input from the ignition source. Experience has shown that this criterion is satisfied within one smolder wave thickness from the irradiated surface in a one-$g_0$ environment. Typical smolder wave thickness in flexible open-cell polyurethane foam under one-g natural convection conditions is approximately 3 cm. Therefore a sample length of 15 cm is approximately 5 wave thicknesses in length;

(ii) In order to obtain accurate representation of the smolder wave profile in the vicinity of the extinguishment limit, a large sample length is required. Smolder wave thickness is anticipated to increase as the reduced-g artificial buoyancy driven flow rate through the porous material is reduced below the natural convection (one-g) limit;

(iii) Physical constraints associated with the Combustion Facility chamber will not allow for sample length much larger than that conceived at present;

(iv) Since rotation of the cannisters produces a centrifugal acceleration on the material sample, equal to $r\omega^2$, and this centrifugal acceleration is a function of radial distance along the sample, the simulated reduced-g environment acting on the sample varies linearly along the sample length. The variation of this simulated g-acceleration along the sample length is not really a problem. Considering a radius arm of 27 cm from hollow shaft centerline to the extreme end of the material sample and a radius arm of 12 cm from shaft centerline to the near end of the sample the following angular velocities are required to produce a given centrifugal acceleration at the extreme end of the sample.

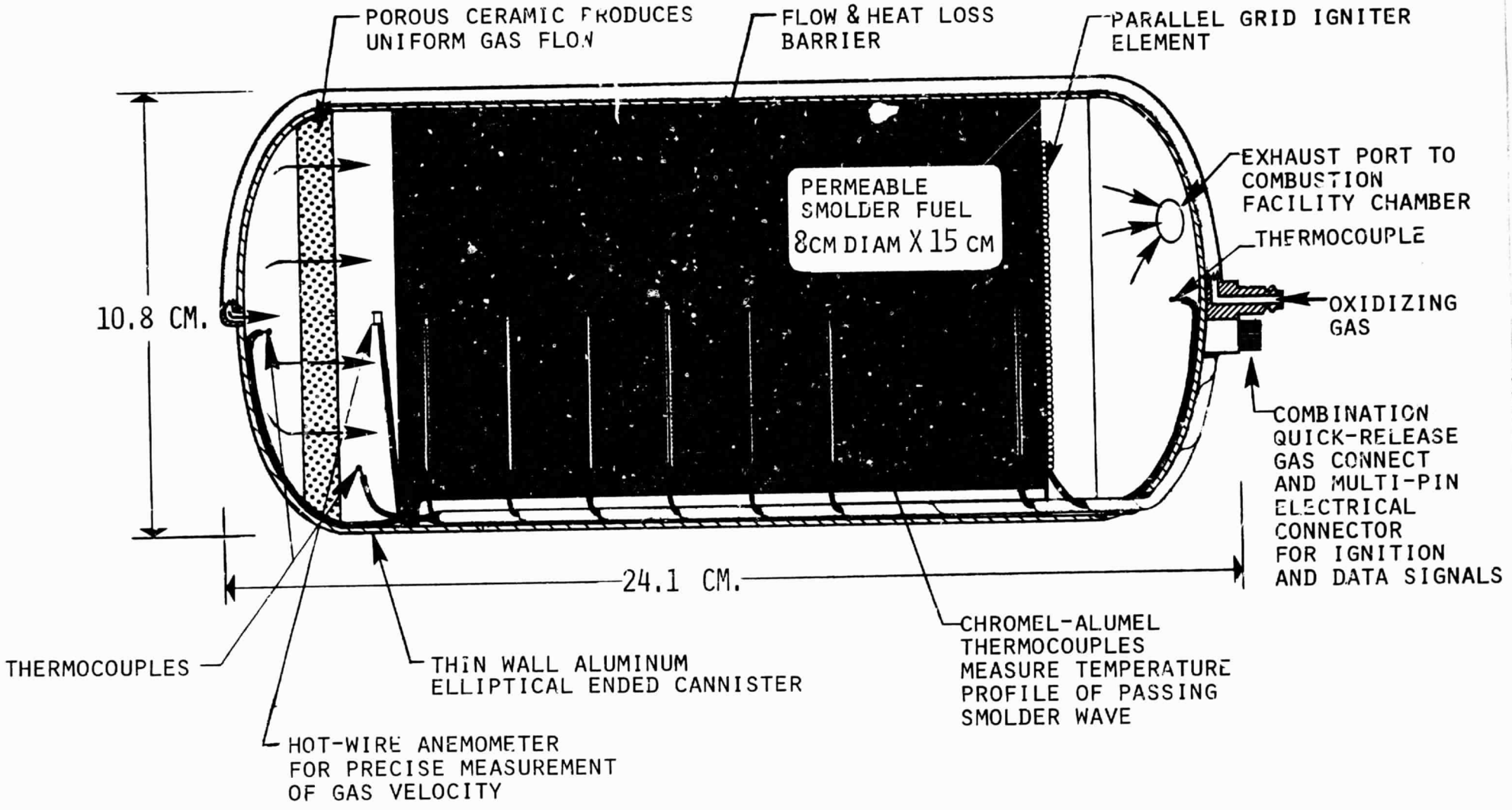


Figure 11. Design Features of Forced-Convection Cannister.

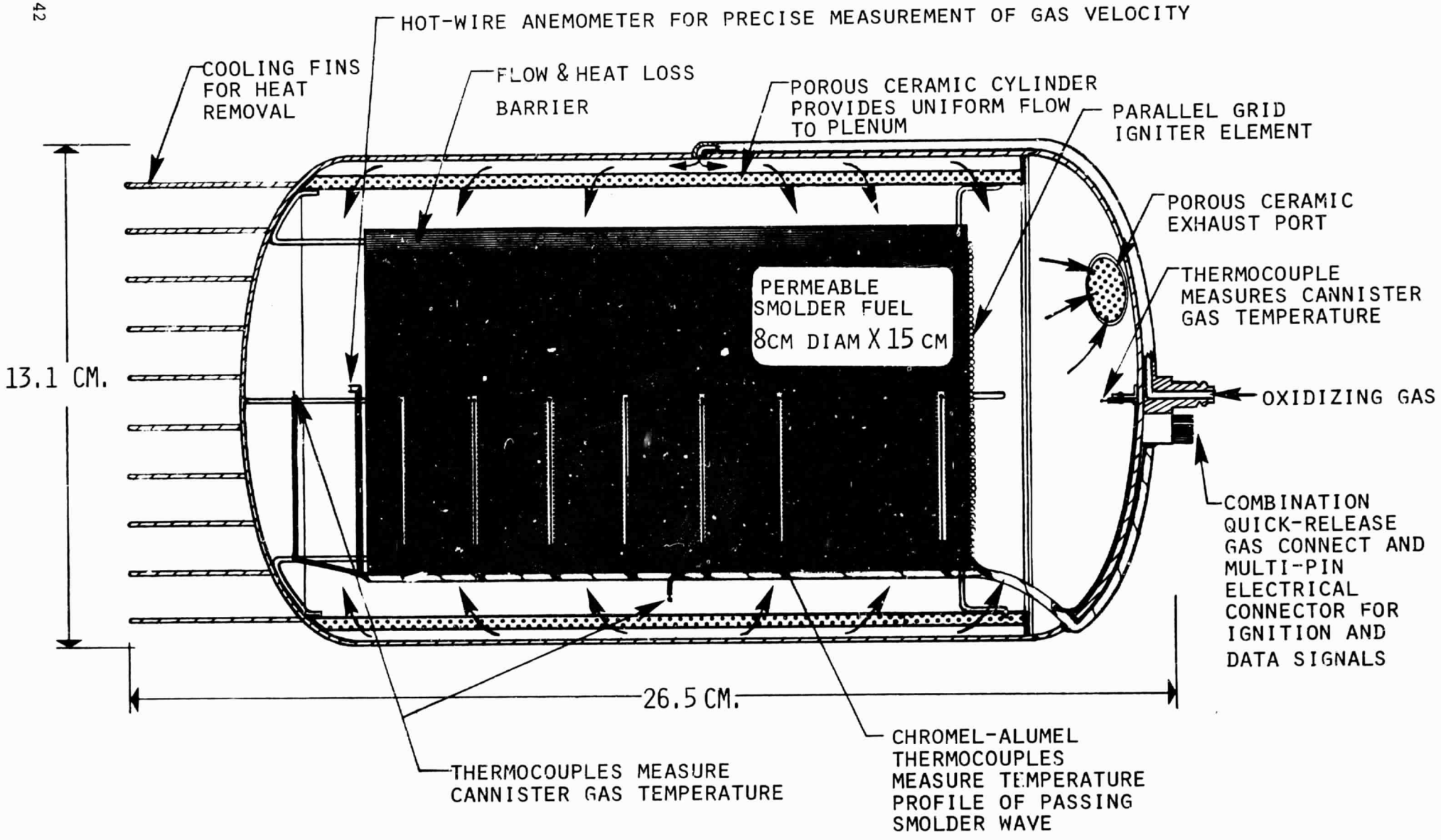


Figure 12. Design Features of Free-Convection Cannister.

for $a_r = 0.25\ g_0$, $\omega = 28.8$ rpm

for $a_r = 0.50\ g_0$, $\omega = 40.7$ rpm

for $a_r = 0.75\ g_0$, $\omega = 49.8$ rpm

In all instances the g-difference along the sample length is 56%. This can be taken into account as a variable parameter in the equations governing smolder propagation, just as other variable parameters (e.g. permeability, gas density, etc.) are taken into account. The buoyancy drive appearing as the difference between the integrated column "head" outside the cannister and that inside the cannister will also vary as the flame front moves along the axis. This will have to be recognized in the mathematical analysis. The appropriate treatment of this buoyancy drive insofar as its impact on smolder wave propagation characteristics should be investigated early in the effort of placing the smoldering conbustion experiment onboard Spacelab.

(v) Appropriate determination of the temperature distribution of the propagating smolder wave requires proper placement of thermocouples along the length of the sample and sufficient sampling of the thermocouple output as a function of time. This has direct implications on the data acquisition system and data multiplexing.

The porous smolder sample is located inside a thin-walled aluminum elliptical-ended cannister, held within a gas flow and heat loss barrier (foamed glass). In order to reduce the possible boundary effects on the smolder combustion wave within the porous sample, a sample diameter of 8 cm was chosen. Each cannister is equipped with a series of chromel-alumel thermocouples to measure the temperature-time-distance characteristics associated with the propagating smolder wave. Use of a hot-wire anemometer is contemplated for placement immediately behind the diffusing screen to obtain a precise measurement of the gas velocity entering the porous sample. A ceramic exhaust port is to be provided in each cannister to allow for withdrawal of combustion gases from the cannister with a direct dump into the "atmosphere" of the Combustion Facility chamber. For ease of assembly and disassembly a combination miniature quick-release gas connect and multi-pin electrical connector for ignition and data signals is provided on each cannister. A parallel grid igniter element, a detail of which is shown in Figure 13, is provided for ignition of the porous smolder specimen. Design features of the Forced Convection Cannister (no rotation of supporting structure and therefore no reduced-g buoyancy driven flow) have been established. Although conceptual design features of the Free-Convection Cannister are displayed in Figure 12, this cannister remains a Critical Component Design, as discussed in Section 3.

The operation of the Forced Convection Cannister is rather straight-forward. A metered flow of oxidizing gas comprised of $O_2/N_2$ in prescribed ratio enters the cannister on the outboard end, and flows through a diffusing screen to ensure uniform gas flow into the porous smolder material. As shown in Figure 11, ignition takes place on the inboard end, thus representing the co-current smolder mode. Product gases from the smolder decomposition

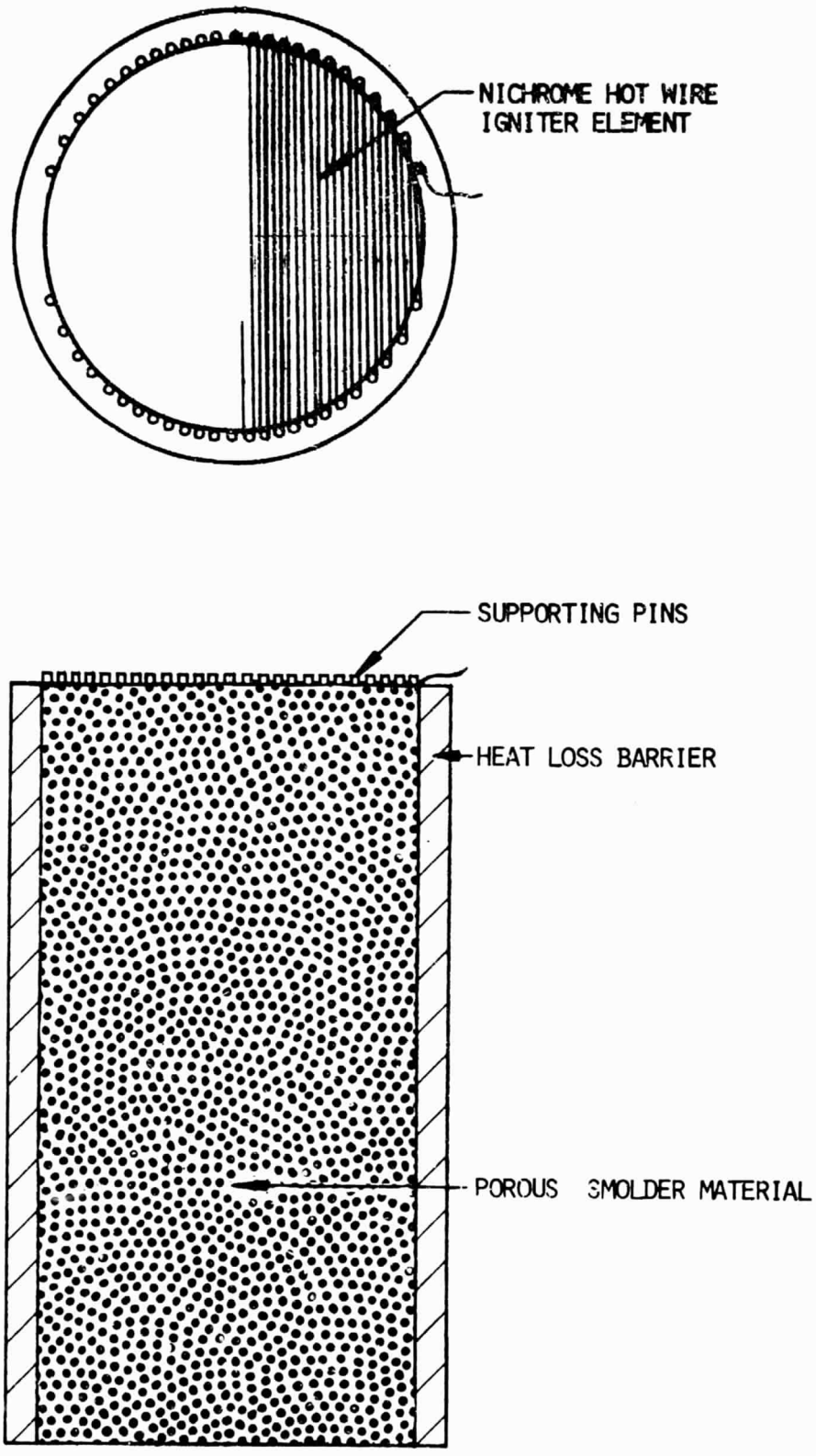


Figure 13. Smolder Material with Proposed Hot Wire Igniter Element.

reaction are swept through the porous material and out the exhaust port by the forced flow of oxidizing gas. The mass outflow rate is equal to the mass inflow rate plus the mass generation rate associated with smoldering combustion. Other Forced Flow Cannisters will be designed to investigate the counter-current mode of smoldering combustion, where both ignition and oxidizing gas inflow occur on the outboard side of the cannister.

This Forced Convection Cannister configuration eliminates any natural pumping action associated with the combustion zone, i.e., no buoyancy driven flow is established associated with a reduced-g field, since the cannister is non-rotating. Therefore the forced flow rate of oxidizing gas establishes the heat release rate in the reaction zone to drive the smolder wave. A controlled reduction in the forced flow rate or reduction of the $O_2/N_2$ ratio of the oxidizing gas will establish driving conditions under which sustained propagation of the smolder wave ceases, i.e. the extinction limit is established. This extinction limit as so obtained should not be confused with that obtained from experiments performed using the free convection cannister since the latter corresponds to a reduced-g buoyancy driven flow situation in which a coupling exists between the natural convective pumping flow rate through the porous body and the heat release rate from the reaction zone. These two physical situations are depicted in block diagram form below.

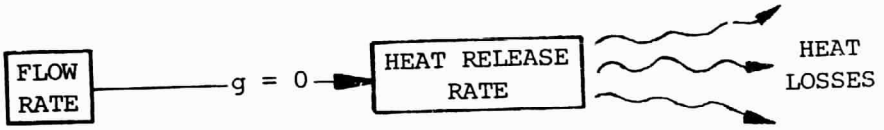


1. Forced Convection

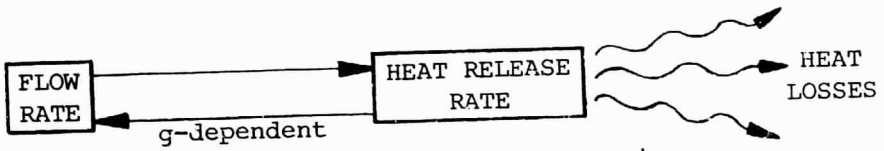


2. Buoyancy Driven Convection

Since the smolder process is oxygen-starved, i.e., all available oxygen is consumed during smoldering combustion, at least up to $O_2/N_2$ ratios of 40%/60% by volume, the rate at which oxygen is delivered to the reaction zone in forced convection experiments determines the rate at which degradation of the foam and heat release associated with the chemical process proceeds. Thus the imposed flow rate establishes the rate of reaction and a unique smolder wave propagation velocity is determinable when proper account of the various heat loss mechanisms is taken.

In a buoyancy-driven convective flow, in the Free-Convection Cannister where the magnitude of the reduced-g driving force is established by the rotational velocity of the cannister, the temperature of the gas within the porous body compared with the temperature of the gas in the annulus surrounding the body

establishes the driving density difference for convective flow. The convective flow velocity through the porous body and ultimately the smolder wave propagation velocity are intimately coupled through a feedback mechanism between the flow rate and heat generation rate. The manner in which the heat generation rate alters or augments the convective flow through the porous body is g-dependent. In the vicinity of the extinction limit this coupling becomes crucial.

The Free-Convection Cannister provides a low velocity scavenging flow to purge the combustion products from the cannister and thereby provides a constant replenishment of the oxidizing gas environment in the annular region surrounding the porous sample. Extreme care must be exercised to ensure proper mixing in the annular region without disturbing the established pressure gradient and convective flow pattern. Design details are presented in Section 3.

This cannister configuration will be used also in a non-rotating experiment (no buoyancy-driven flow, no forced flow) to determine whether smoldering can occur with only diffusion driving the flow, i.e., "Fick's Law" type flow. In principle, such smolder should occur; in practice, because such flow rate is expected to be quite low, heat losses may quench diffusion smolder.

It should be noted that a combined forced convection-buoyancy driven convection cannister was originally contemplated. However, this cannister design has been abandoned since the usefulness of data obtained from such an experiment in an attempt to extract critical parameters pertaining to the transport mechanisms is in question. The use of such an experimental configuration in establishing a fundamental understanding of the smolder combustion process in the neighborhood of the smolder extinction limit is debatable.

## 2.3 Definition of Matrix of Test Variables

Before deciding on the test matrix to be performed on Spacelab and the ultimate strategy of the test sequence to accomplish the tests required by the matrix, physical variables that affect the smolder process must be identified. These include the physical material itself and associated physical characteristics such as permeability, chemical composition, porosity, structure (flexible, open-cell vs. granular); shape, size, and confinement of the test material; $O_2/N_2$ ratio of the oxidizing gas; simulated g-level (and therefore magnitude of buoyancy-driven flow velocity through sample); forced air mass flow rate (forced convection); pressure level in cannister; counter-current and co-current configurations; and temperature of oxidizing gas. It has previously been stated that the temperature of the oxidizing gas cannot be independently controlled within the Combustion Facility Chamber, as presently planned by NASA. The possibility of incorporating controllable heater elements in the feed line to the individual cannisters should be investigated. The relative importance of temperature of the oxidizing gas as an independent variable will have to be investigated by laboratory experiments.

The variables identified above have been shown to affect the smolder process. The number of tests to be performed must be able to be accommodated within the time constraints imposed and must provide sufficient data necessary for characterization of the smolder wave structure in the neighborhood of the extinguishment limit.

In order to maximize the number of tests in the time available we presently plan to assemble 32 cannisters (8 tiers of 4 cannisters each) within the Combustion Facility Chamber and execute four successive test runs without entering the chamber again except for disassembly. One tier on each half-shaft will be ignited simultaneously. This corresponds to eight smolder combustion tests performed at the same reduced gravity level. Four fractional $g_0$ levels have been chosen for experimentation: zero-g (no rotation, Forced Convection; and no rotation, Pure Diffusion) 0.25 $g_0$, 0.50 $g_0$ and 0.75 $g_0$. The test matrix as presently conceived is presented in Figure 14.

## 2.4 Choice of Smolder Material(s)

The choice of material(s) to be investigated for smoldering combustion experiments in the Combustion Facility onboard Spacelab is dictated by several requirements. First, the material must be able to support smoldering combustion in a self-sustaining mode, as determined by ground-based laboratory experiments. Second, supporting data from ground-based laboratory experiments conducted on the specific material(s) should exist to provide the data base necessary for comparison with Spacelab experiments, e.g., temperature profiles, smolder wave velocity as a function of various parameters. Third, the physical and thermochemical properties of the material must be accurately known or determinable and any tendencies for material structural breakdown and possible reorientation under mechanical stress must be minimal.

We have identified several general categories of candidate materials.

(i) Cellulosic materials, either commercially available cellulosic cylindrical elements, 99.5% pure α-cellulose; or granulated cellulosic material such as shredded and fluffed paper, sawdust, or tobacco; or porous wood fiberboard.

(ii) Polyurethane foams, either flexible or rigid, but permeable.

(iii) Phenol Formaldehyde foams, either rigid or granulated.

(iv) Polyisocyanurates.

(v) Polystyrenes or Polyethylenes

(vi) Urea Formaldehyde

| FORCED CONVECTION | | BUOYANCY DRIVEN CONVECTION | | PURE DIFFUSION | |
|---|---|---|---|---|---|
| NUMBER OF CONDITIONS | PARAMETER | NUMBER OF CONDITIONS | PARAMETER | NUMBER OF CONDITIONS | PARAMETER |
| 1 (g = 0) | g | *3 (g = 0.25,0.50, 0.75 $g_0$) | g | 1 (g = 0) | g |
| 1 (p = 1 atm) | p | 1 (p = 1 atm) | p | 1 (p = 1 atm) | p |
| 1 | PERMEABILITY | 2 | PERMEABILITY | 2 | PERMEABILITY |
| 2 | $O_2/N_2$ RATIO {20%/80% 40%/60% | 2 | $O_2/N_2$ RATIO {20%/80% 40%/60% | 2 | $O_2/N_2$ RATIO {20%/80% 40%/60% |
| 2 | $\dot{m}_g$ {0.1 cm/sec 0.5 cm/sec | | | | |
| 2 (co-current, counter-current) | PROPAGATION DIRECTION | 2 (co-current, counter-current) | PROPAGATION DIRECTION | 1 | PROPAGATION DIRECTION |
| 8 TOTAL | | 20 TOTAL | | 4 TOTAL | |

*Note: The 0.50 $g_0$ condition will be conducted in two stages. Only permeability and $O_2/N_2$ ratio will be varied for the 0.50 $g_0$ condition, propagation direction being co-current. Thus only 4 tests at this reduced-$g_0$ condition are planned. This is necessary to accomodate the 4 pure diffusion zero-g smolder tests. If smolder does not take hold and propagate after ignition in these pure diffusion tests, the cannister will be spun up to 0.50 $g_0$ and the counter-current propagation mode will be tested.

Figure 14. Matrix of Planned Experiments within Imposed Time Constraints

Cellulosic materials - Our literature search reveals that theoretical and experimental investigations of the mechanism of smoldering in cellulosic materials (commercially available cylindrical cellulosic elements and 99.5% pure α-cellulose) have been conducted.[32] Smoldering has been observed in quiescent (natural convection) oxygen/nitrogen environments of various pressures and compositions. Extinguishment limits are established for various combinations of oxygen mole fraction and partial pressure. It is not clear whether uniformity of composition of certain cellulosic materials can be achieved, especially when considering such material as sawdust, shredded and fluffed paper, and porous wood fiberboard. Such granular or shredded cellulosics as paper, tobacco, and sawdust have been ruled out due to nonuniformities of material and variabilities inherent in packing density (thereby affecting permeability of the sample). A photograph of a fluffed cellulosic material is shown in Figure 15c.

Polyurethane Foams - Extensive experimental data exist on smoldering of open cell flexible polyurethane foams, conducted by Dr. Martin Summerfield and associates at Princeton University.[48] These ground-based free convection and forced convection experiments serve as the technological data base for the proposed smoldering experiments to be conducted in the Combustion Facility in Spacelab. It has been found experimentally that certain flexible polyurethane foams will not smolder without assist, i.e., fabric covering required on ignition surface, much like an upholstery cover. These are ruled out as possible candidate materials unless we find that pre-heating the oxidizing gas takes care of the problem. It should also be pointed out that the majority of experiments conducted with flexible polyurethane foams were performed in the co-current mode, i.e., in a frame of reference fixed to the propagating smolder front, fuel and oxidizer are seen to approach the reaction zone from the same direction. A few attempts to achieve a steady, sustained smoldering process with flexible polyurethane foams in the counter-current mode, i.e., in a frame of reference fixed to the smolder front, fuel and oxidizer are seen to approach the reaction zone from opposite directions, resulted in extinction of smolder due to the formation of a melt (tar) as a product of smoldering combustion rather than a char. The cell structure in the melt zone is closed and, as a result, the smoldering process becomes oxygen starved. These competing degradation pathways, char or melt, in polyurethane foams are sensitive to the rate at which virgin foam material is heated. Certain flexible polyurethane foams are biased toward dominance of char formation and these therefore will be possible candidates for space experimentation.

Another possibility for choice of polyurethane material in which the smoldering process favors the char formation pathway is a permeable rigid foam. The tendency toward cell degradation in the counter-current mode is reduced, thereby reducing the possibility of melt (tar) formation. Candidate materials in this category are being explored but the existing data base is limited.

Phenol Formaldehyde Foams - These are commercially available as rigid foams. This foam is a low permeability fuel in which the pore structure is too fine to permit significant flow-through of air under the influence of buoyancy forces (natural convection) alone. Ground-based experiments verify that only surface smolder results in a natural convection environment. When fuel permeability to air inflow is low, oxygen access is essentially limited to whatever penetration depth diffusion can provide. This will in turn depend on

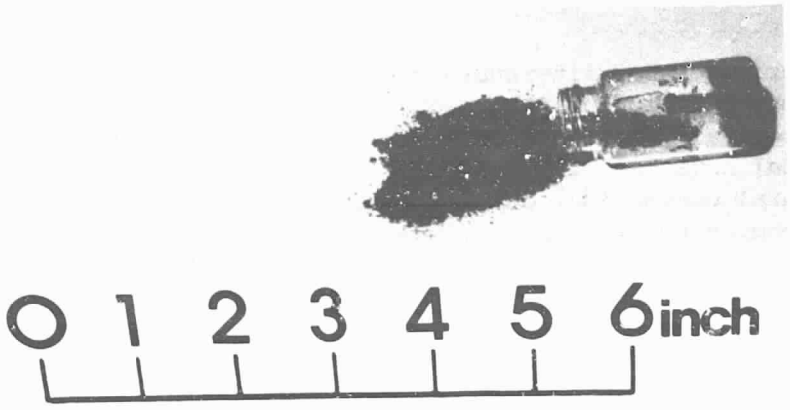


(a) Granulated Polyisocyanurate

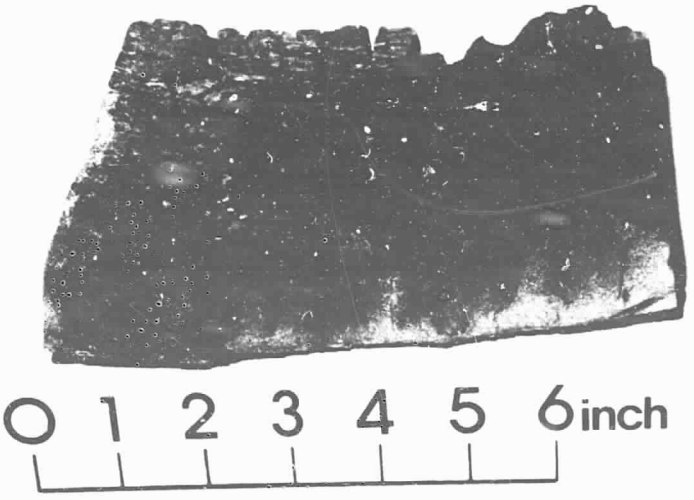


(b) Rigid Phenol Formaldehyde Foam, Showing Surface Fissuring

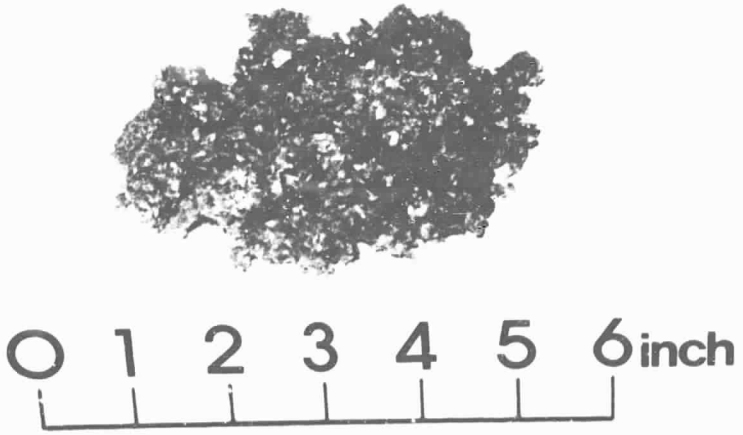




(c) Fluffed Cellulosic

Figure 15. Photographs of Candidate Smolder Materials.

the porosity of the fuel. The chief concern of utilizing phenol formaldehyde foam for smoldering studies is its tendency toward surface fissuring during heating, whether in a natural convection or forced convection environment. This is an inherent characteristic of this low permeability fuel and is most likely attributable to mechanical stress. The process of surface fissuring occurs during the ignition phase of smolder initiation by an external thermal source and can be a continuous aspect of the surface smolder process. These cracks can have a major impact on the tendency to smolder and on smolder rates because they are low resistance access routes for oxygen penetration into the fuel. Also, radiation from the ignition source can penetrate the surface in an irreproducible way, and char can react exothermically to an extent that depends on the local oxygen concentration and gas flow pattern. The physics of crack formation and propagation during the smolder process in this low permeability fuel may so complicate the theoretical modeling efforts that fundamental understanding of the smolder process itself may become obscured. Therefore, if indeed a phenol formaldehyde foam is chosen as a candidate material, we would try to eliminate this tendency toward surface fissuring by going to a recast granulated material in which the permeability is purposefully increased by the use of suitable blowing agents. In this form the material should be an excellent char-former in the counter-current smolder mode. Note that a pure granulated phenol formaldehyde material presents additional problems associated with variabilities inherent in packing density and the effect of super-g levels experienced by the packed granulated material during launch of the Shuttle. A photograph of rigid phenol formaldehyde foam is shown in Figure 15b.

Isocyanurates - Granulated polyisocyanurates have been demonstrated to undergo smoldering combustion in forced flow experiments in a Buchner funnel. As was the case with granulated phenol formaldehyde, internal cementing of the material may be required to ensure uniformity of packing density. A photograph of granulated polyisocyanurates is shown in Figure 15a.

Polystyrenes or Polypropylenes - These are unacceptable as candidate materials for smoldering experiments since they behave thermoplastically, i.e., the degradation pathway is such that a pure melt or liquid results; char formation and therefore a sustained smolder wave does not result.

Urea Formaldehyde - These types of foams, commonly used for insulation purposes, may have to be ruled out as possible candidates for smoldering materials. This is based entirely on recent controversy as to the toxicity of formaldehyde fumes and because one of the smoldering combustion products is hydrogen cyanide. Of course, since the proposed Spacelab apparatus is a completely sealed one, the question of toxicity deserves discussion.

A tabulation of some of the relevant properties of various candidate smolder materials is presented in Figure 16.

Because of the extensive data base that exists from ground-based experiments on flexible, open-cell polyurethane foams and our own familiarity with smoldering properties of this material at 1 $g_0$, it is our recommendation that this be the candidate material for smoldering combustion experiments.

| MATERIAL | SPECIFIC HEAT kJ/kg°K (cal/g C) | THERMAL CONDUCTIVITY $10^{-2}$W/m°K ($10^{-4}$cal/sec cm C) | MINIMUM IGNITION TEMPERATURE K | MINIMUM IGNITION ENERGY J | HEAT OF COMBUSTION kJ/g (kcal/g) | STOICHIOMETRIC FLAME TEMPERATURE K |
|---|---|---|---|---|---|---|
| POLYURETHANE FOAM | 1.68-1.89 (0.40-0.45) | 6.3-31.1 (1.5-7.4) | 710 | 0.020 | 23.9 (5.7) | 2370 |
| PHENOL FORMALDEHYDE FOAM | 1.60-1.76 (0.38-0.42) | 12.6-25.2 (3.0-6.0) | 940 | 0.030 | 28.1 (6.7) | 2130 |
| UREA FORMALDEHYDE FOAM | 1.68 (0.40) | 29.4-42.0 (7.0-10.0) | 800 | 0.900 | 18.1 (4.3) | 2220 |
| CELLULOSE ACETATE | 1.26-2.10 (0.30-0.50) | 16.8-33.6 (4.0-8.0) | 690 | 0.040 | 16.8 (4.0) | ---- |

NOTE: For Flexible, Open-Cell Polyurethane Foam, H2528
$Q_c$ = 32.3 kJ/g (7.7 kcal/g)

*Note: Obtained from Flammability Handbook for Plastics, C. Hilado (ed.), 1974.

Figure 16. Tabulation of Properties of Various Candidate Smolder Materials

## 2.5 Identification of Subsystems

Many of the various subsystems identified at the beginning of Section 2 have been discussed in depth in Section 2.2 "Conceptual Experiment Configuration Design". Remaining subsystems are discussed below.

### 2.5.1 Initiation of Smoldering; Ignition System

Initiation of smoldering may be accomplished by several means. Moussa, et al[32], conducted an experimental investigation of the mechanism of smoldering in cellulose materials in which smoldering was initiated by bringing an electric heating coil in contact with one surface of the specimen. The heating coil provided approximately 4.2 J/cm$^2$-sec (1.0 cal/cm$^2$-sec) heat flux to the sample surface. The duration of input heat flux was quite arbitrary, governed by the visible appearance of the onset of a spreading smolder wave.

Summerfield, et al[48], of Princeton University employed a high intensity Tungsten lamp focused on a one-inch diameter blackened circle (C black) on the surface of an 11.4 cm (4.5 in) diameter sample of flexible polyurethane foam. This radiation source was used only to initiate smolder to a self-sustaining condition, requiring a flux of 0.92 J/cm$^2$-sec (0.22 cal/cm$^2$-sec), sustained for 6-8 minutes. No attempt was made to "overdrive" the smolder wave by providing for sustained radiation input during the smolder wave propagating phase.

In other studies conducted by the Princeton group, smoldering combustion in flexible polyurethane foams was initiated by a smoldering fabric cover placed in contact with the upper surface of the foam specimen. The thrust of this investigation was to examine the extent and hazard of smoldering in upholstered furniture. Therefore, no advantage is seen to adopting this means of initiation for the proposed space experimentation.

One of the prime disadvantages of utilizing a point source as a means of initiating smolder is that the ensuing smolder wave propagation cannot be treated by a one-dimensional theoretical formulation. Indeed, it has been determined[48] that the propagation speed of the smolder wave at the surface is considerably different from that in the interior of the sample. (Figure 17) Thus, from the point of view of utilizing the data effectively in a theoretical model uncomplicated by multi-dimensional effects, the ignition system was modified in attempt to achieve uniform heat flux over the entire exposed surface of the sample. A commercially available 0.159-cm (0.0625-in) diameter Nichrome wire coil heater wound with constant radial pitch (Archimedian spiral) was substituted as the ignition source. Unfortunately, in the limited trials, uniform surface ignition was not achieved because of non-uniform surface heating with radial distance from the center of the circular face of the cylindrical specimen. This can be overcome by the use of a spirally wound wire with decreasing radial pitch.

It should be noted that the incident heat flux is a sensitive parameter. When the incident flux exceeds 1.26 J/cm$^2$-sec (0.3 cal/cm$^2$-sec), the polyurethane foam appears to melt (tar) rather than form the char which is the basis for

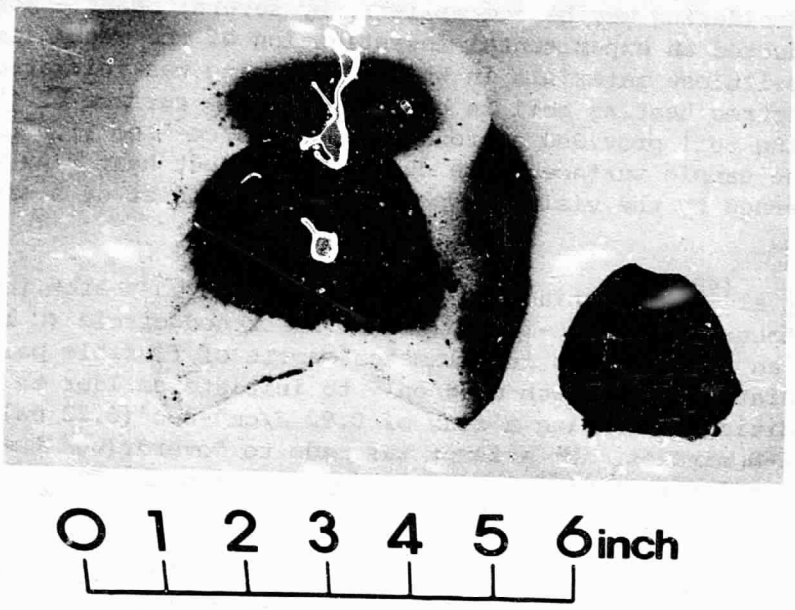




Figure 17. Photograph of Char Formation in Flexible, Open-Cell Polyurethane Foam, Resulting From Point Source Ignition.

smolder. This is quite instructive since it suggests competing degradation pathways in the polyurethane foam whose competition is sensitive to the rate at which the foam is heated.

Bowes and Thomas[10] in their experimental self-heating and ignition studies conducted with 27-72 B.S. Sieve fraction of mixed hardwood sawdust packed into cube-shaped wire baskets at a density of 0.26 g/cm$^3$ achieved ignition by suspending the basket in an oven at controllable temperature levels. The oven temperature was increased in steps of 5 degrees C until the temperature was found at which ignition of the sample occurred. Ignition temperature was defined as that point in the temperature-time history of a thermocouple located at the center of the specimen at which an inflection point exists. After ignition the oven temperature was maintained constant at this "ignition" temperature, thereby providing a constant temperature environment for the specimen. This is essentially a self-heating process. The conditioning oven also provided a means of controlling the temperature of the forced flow air supply to the sample. The temperature pre-conditioning of the inflowing air also aids the smoldering process.

Self-heating and ignition of porous carbonaceous material was studied by Shea and Hsu[45] in which a conditioning oven was also used to heat the sample to the ignition temperature.

In the smoldering combustion studies with dust trains (cork dust, grass dust, commercially mixed wood sawdust, and rigid porous wood fiberboard) conducted by Palmer[41], smoldering was initiated by a small flame applied to the end of the dust train or applied across the entire width of the unsupported end of a strip of porous wood fiberboard, for a period of 0 to 1 minute.

Based on this review of the literature on the ignition source utilized in various experimental smoldering studies we propose the following ignition system for smoldering experiments to be conducted onboard Spacelab. Driven by the need for simplicity of design and operation, the requirement of uniform heat flux from the ignition source to the exposed surface of the porous smolder material, and a degradation pathway for the candidate materials that is critically dependent upon the level of incident flux, we have chosen to use a parallel-grid Nichrome wire igniter. We envision the grid to be mounted on ceramic pins embedded in the end of an insulating sleeve surrounding the candidate smolder material. The preliminary design of the parallel-grid wire igniter is shown in Figure 13. This arrangement provides for ease of construction, uniform heating of the material surface, and rigid support of the igniter element thereby guarding against deformations that may occur during super-g levels experienced during Shuttle lift-off. Wire diameter, resistance per unit length, applied voltage, and gap spacing between grid wires and sample surface are parameters that must be established to provide the necessary level of heat flux to the sample to ensure initiation of the smoldering process. For a given Nichrome wire diameter and length, the Joule heating of the wire becomes a function of the applied voltage and, for a fixed gap spacing, the heat flux delivered to the sample surface can be determined. The flux values can be obtained by use of a water-cooled Hy-Cal #C-1119 Calorimeter consisting of a differential thermocouple under a disc of 0.3175-cm (0.125-in) diameter. These calorimetric studies are necessary

ground-based experiments which must be conducted in order to ensure that the heat flux delivered to the surface lies within the corridor for avoidance of melt formation. Circuitry must be provided to maintain a constant incident flux.

In order to preclude the possibility of over-driving the initiated smolder wave, i.e., acceleration of the wave front, the time duration for thermal radiation to the surface must be independently controlled, again requiring the need for ground-based experimentation with this proposed igniter design. Either a simple timing circuit or a more complicated feedback circuit sensitive to critical parameters characteristic of the developing smolder wave are design requirements. It may be possible to develop a threshold for interruption of igniter flux. A control circuit is proposed consisting of a simple "AND" gate. Inputs to the gate circuit would be (i) the temperature in the smolder material as sensed by a thermocouple embedded below the exposed surface, and (ii) a phototransistor/light source combination sensing the smoke level in the exhaust gases. Since the maximum temperature in the smolder wave of polyurethane foams, for instance, is seen to be in the range of 620 K to 770 K (350 C to 500 C) dependent on the forced air flow velocity and the percent oxygen of the oxidizing gas and since the smoldering process, once initiated, liberates considerable smoke, these two criteria can be used in establishing a threshold cut-off for incident thermal radiation.

### 2.5.2 Safety Assurance System: $N_2$ Purge

A certain degree of variability in the gaseous and solid products of the smolder process in polyurethane foams has been observed experimentally.[48] The solid char residue is a complex C,H,O,N material. The fraction of foam converted to this char residue is a function of both the heating rate and oxygen availability. The variability of some of the gaseous products of smolder of polyurethane foam is indicated in Figure 5, taken from Reference 48. These results were obtained in a forced convection environment in a Buchner funnel, but with a forced gas flow rate of the same order as natural convection values. Sampling of the product gases was limited to the final product gases as the percentage of oxygen in the forced gas flow was varied.

The most important observation to be made is that all available oxygen is consumed in the smolder process, with the possible exception of 40%/60% $N_2$ gas flow. This is representative of an oxygen-starved process whose extent is limited by the oxygen availability. This could have been inferred directly from temperature and smolder wave propagation velocity measurements of the smolder process for various $O_2/N_2$ gas flow ratios. This is displayed in Figure 7. In this figure smolder velocity is plotted versus percent $O_2$ in the flowing gas for two different gas flow velocities. As the percent oxygen in the gas flow is increased, the smolder velocity increases linearly with a corresponding increase in maximum smolder wave temperature. The smolder process in air (21% $O_2$) lies near the smolder extinction limit, while for 50-60% oxygenated air, flaming ensues. Therefore as more oxygen is made available, the smolder process becomes faster, hotter and more complete.

The smolder product gases sampled in Figure 5 are $O_2$, CO, and $CO_2$. An increase in the $O_2/N_2$ ratio, resulting in increased temperature of the smolder wave, is accompanied by an increase in the oxidized product gases CO and $CO_2$. Clearly the CO concentration must achieve a maximum and then decay to zero as available oxygen increases toward the stoichiometric amount. It is the generation of CO that concerns us from a safety standpoint. At present, the smoldering combustion experiments to be conducted onboard Spacelab call for a continuous scavenging of the combustion products from each cannister and continuous $O_2/N_2$ gas replenishment. Therefore mixing of the carbon monoxide product gas and oxygen from the replenished air supply must be considered. Mixtures of carbon monoxide and oxygen exhibit flammability limits. From practical experience it is known that explosive gases may be rendered nonflammable, that is, incapable of sustaining combustion, by addition of diluent gases in sufficient quantity. Such diluents may consist of excess fuel, or excess oxidant, or inert gases, and standardized experimental procedures are in use to determine the quantity of diluent that must be added to a fuel-oxidant mixture to render the mixture nonflammable. Limits of flammability are thus defined by experimentally determined mixture compositions. These experimentally determined limits are proven to be reliable for safety considerations.

The effect of additions of $N_2$ diluent on the fuel (CO)-oxygen ratio of flammability limit mixtures is presented in Figure 18, for room temperature and atmospheric pressure. This figure shows compositions of limit mixtures of CO plus air plus $N_2$ diluent gas in excess of the nitrogen in the air. These limits have been determined by standard Bureau of Mines' procedures and the figure is reproduced from Reference 49. Outside the area enclosed by the limit curve the mixtures do not propagate flame. The mixture at the extreme tip of the area contains the maximum amount of diluent of any flammable mixture and also the percentage of oxygen below which flammability is impossible. For example, in the case of carbon monoxide in air diluted with $N_2$, the mixture is nonflammable when the percentage of $N_2$ in air exceeds 70%, regardless of the concentration of CO, or when the percentage of $O_2$ in the $N_2$-air mixture is below 6.5%. The maximum safe percentage of oxygen in mixtures of carbon monoxide with air and $N_2$ diluent at room temperature and one atmosphere pressure is tabulated in Reference 49 as 5.6%.

The proposed smoldering experiment design provides for scavenging the smolder combustion products from the individual cannisters into the plenum (chamber) of the Combustion Facility and replenishment of the oxidizing environment in each cannister at a rate commensurate with natural (one-g) convection flow rates. Blow-by of the oxidizing gas around the smolder material is anticipated since the smolder material represents a high resistance path for the flow. Therefore, the exhaust gas from the cannister may be considered vitiated air, i.e., a mixture of smolder combustion products and oxidizing gas. In light of the foregoing discussion on flammability limits of CO plus air plus $N_2$ diluent gas, it is recommended that a continuous purge of $N_2$ gas be fed into the plenum such that the percentage of $N_2$ in the vitiated exhaust gas from the cannisters equals 70%, and the pressure of the plenum is maintained at the prescribed level. The experiment will thereby qualify as "safe" from an exhaust products' reactivity standpoint.

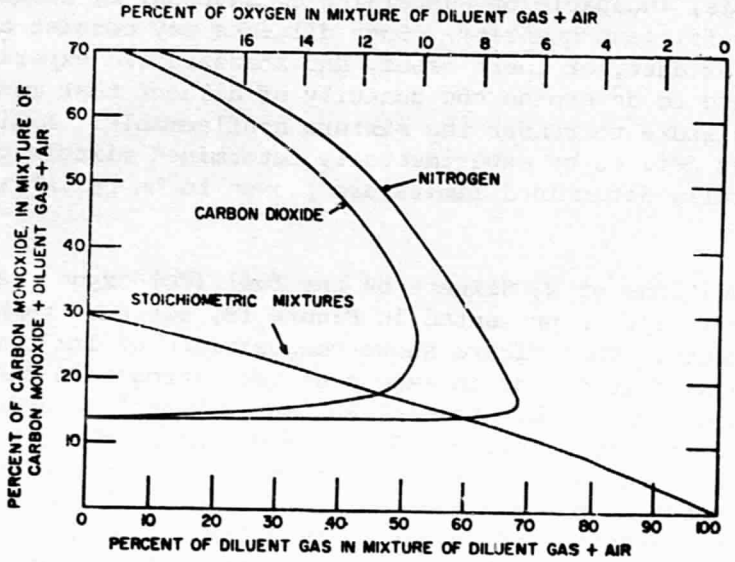


Figure 18. Limits of flammability of carbon monoxide in air diluted with $CO_2$ or $N_2$. Mixtures saturated with water vapor. Room temperature and atmospheric pressure.

Assuming a replenishment drift velocity through each cannister of 0.1 cm/sec, corresponding to a volumetric scavenging outflow rate of approximately 9.0 $cm^3$/sec (flow rate through porous body augmented by gas production due to smoldering combustion), we have a total outflow rate into the Combustion Facility of 72.0 $cm^3$/sec. This assumes that 8 cannisters undergo reduced-g smolder experiments at a given time. If we further assume the case of an initial air environment in the Facility Chamber then the requirement of 70% $N_2$ by volume in the Chamber requires a volumetric flow rate of pure $N_2$ into the Chamber of 2.33 times that of the vitiated effluent volumetric flow rate. This can be seen to be the case since

$$[N_2] \; / \; [N_2 + \text{effluent}] = 0.7$$

or

$$[N_2] = \frac{0.7}{0.3} \; [\text{effluent}] = 2.33 \; [\text{effluent}]$$

or

$$\dot{V}_{N_2} = 167.8 \text{ cm}^3/\text{s}$$

Since typical smolder velocities are ca. $0.5 \times 10^{-2}$ cm/sec and the sample lengths considered are 15 cm, the time for the smolder wave to reach the end of the sample is 50 min. Allowing for an ignition transient time typically of 5 min. duration, this requires a total test time of 55 min. and, therefore, $5.5 \times 10^5$ $cm^3$ $N_2$ gas. Note that a typical laboratory $N_2$ gas bottle pressurized to 170 atm contains $6.78 \times 10^6$ $cm^3$ $N_2$. Since 4 sets of experiments are planned, each set comprising 8 cannister tests, the total $N_2$ requirement for purging the Combustion Facility Chamber to ensure safety is $2.2 \times 10^6$ $cm^3$. The precise quantity of $N_2$ required (the above is an upper limit for the co-current case) depends on the conditions of each individual test in the experimental matrix. Also, pre-purging of the Combustion Facility Chamber with $N_2$ lowers the overall $N_2$ requirement.

It should be noted that the section entitled "Stoichiometry" indicates that $H_2$ gas may be present as a product gas of smoldering combustion in significant quantities. If further chemical analysis establishes that this is indeed true, then we must concern ourselves with safety aspects of $H_2$ in the Combustion Facility Chamber (flammability limits), in the same way as we have considered CO. The requirement for nitrogen dilution will then depend on what we learn about the fraction of $H_2$ gas in the smolder combustion products.

Finally, the limits of flammability of carbon monoxide in air diluted with $CO_2$ and $N_2$, as presented in Figure 18, are obtained at 1 g. The effect of reduced-g on these flammability limits must be taken into account. It has recently come to our attention, Reference 50, that the flammability limits are widened at reduced-g levels. Therefore, for the case of CO in air diluted with $N_2$ the minimum percentage of $N_2$ diluent necessary to ensure a nonflammable mixture exceeds 70%. These data must be considered in the final design phase. However, the message is clear; safety can be assured.

Various active safety control systems are recommended for incorporation into the smolder experiment package. For fire safety in the individual smolder cannisters we will rely on the microprocessor circuitry, which monitors all the sample thermocouples, to activate a 2-way solenoid valve in the event that $T > 1300$ K ($T_{SMOLDER} \leq 1020$ K), interrupting the flow of oxidizing gas and purging the individual cannisters with $N_2$. Since the smolder process cannot be sustained without replenishment of the oxidizing gas, this ensures extinguishment of the combustion process. Also, as a further safety measure, rotation of the support structure will cease in the event that $T > 1300$ K, as sensed by the microprocessor circuitry, thereby eliminating convective flow associated with the reduced-g environment.

Experiment shut-down procedures to ensure safe handling of the cannisters as the experiment is disassembled in the Combustion Facility Chamber is another area of consideration. When the microprocessor circuitry monitoring the last thermocouple in the smolder sample detects a large negative $\Delta T$, this is a signal that data sampling in the cannister is complete, since the smolder wave front has progressed through the entire sample length. At this point, oxidizing gas flow is interrupted, a $N_2$ purge is initiated and rotation of the experiment ceases. An indicator light will signal to the scientist/ astronaut that the experiment can be safely disassembled.

Flammability of the cannister exhaust gases has been discussed above. It should also be noted that the Combustion Facility Chamber is equipped with a fire-suppression system (Halon 1301).

## 3. Critical Component Design

Three aspects of the proposed smoldering combustion project have been identified as Critical Component Designs. These are as follows:

### 3.1 Reduced-g Buoyancy Driven Convection Flow Smolder Cannisters

The design for this type of cannister (see Figure 12) must allow for scavenging of the smolder combustion product gases from the cannister and replenishment of the "atmosphere" of the cannister with oxidizing gas. In order to establish a reduced-g buoyancy driven convective flow pattern around and thru the sample, an annular clearance volume must be provided between the sample and cannister walls, in an attempt to simulate an "infinite" surrounding gas environment. However, if the gas temperature of the atmosphere surrounding the sample (comprised of combustion gas products and fresh oxidizing gas) equals the average gas temperature within the smolder wave of the porous smolder material, no driving density difference would exist and hence no buoyancy driving force. Therefore the gas temperature in the cannisters is a critical parameter which must be established before design finalization. The possibility of using cooling fins on the rotating cannisters is recommended if, indeed, the gas temperature in the annulus surrounding the smolder sample must be reduced.

Another critical issue associated with the free (natural) convection smolder cannister design is gas flow control and distribution within the cannister to provide for establishment of free convective flow through the permeable smolder fuel sample and to provide appropriate mixing of the smolder combustion product gases with the replenishment oxidizing environment (purge vs. replenishment). The annular clearance surrounding the smolder fuel sample provides the void volume in which the oxidizing atmosphere is maintained and mixing occurs. A schematic flow circuit diagram of the free convection (at reduced-g) smolder cannister is shown in Figure 19.

The cannister design must permit continuous replenishment of the atmosphere in the void surrounding the smolder specimen so as to maintain a sufficient oxygen concentration to permit continuous support of the smolder process in the specimen. For the purpose of this design it was decided to maintain a concentration of $O_2$ at the 20% level, equivalent to the normal atmosphere. The flow circuit must also permit continuous removal of spent air in an amount equal to the inflow of replenishing air. The region outside the porous fuel specimen is treated in this schematic flow circuit diagram as a void in the cannister, considered as a mixing chamber. This mixing chamber receives the flow of replenishment air from the oxidizing gas supply. The excess spent air is withdrawn from the void and dumped into the Combustion Facility Chamber. This flow is marked "vitiated air." The smoldering porous fuel specimen, drawing in some of the surrounding atmosphere gas, is treated as a pump which discharges gas as spent air, "smoke", into the surrounding void volume. This flow system can be considered as operating in a steady-state mode with continuous inflow of replenishing gas, continuous outflow of spent gas, and the porous fuel specimen acting as a continuous pump.

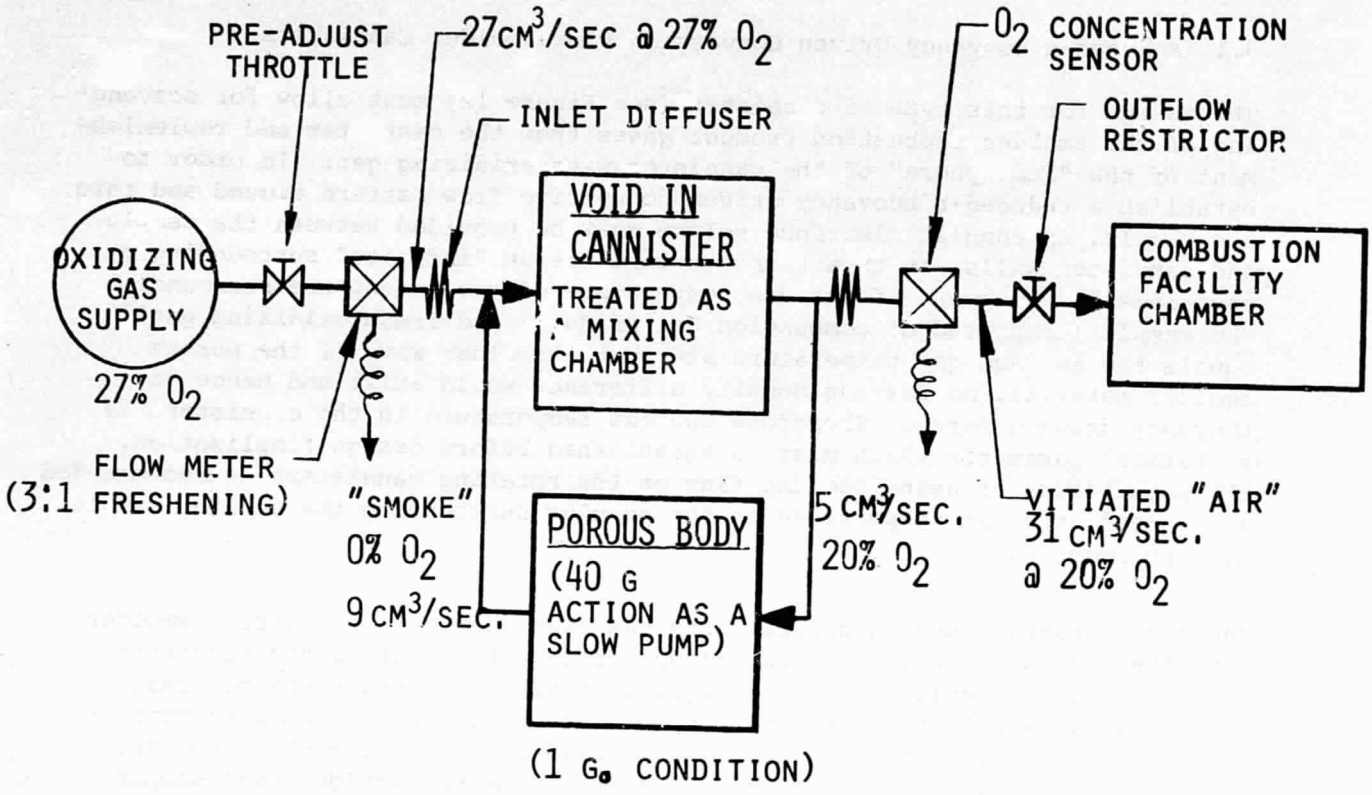


Figure 19. Schematic Flow Circuit of Free-Convection Smolder Experiment.

The quantities shown in the flow circuit diagram are derived as follows. The interior of the porous body of smoldering fuel is estimated to receive oxidizing air in a natural convection mode at the rate of approximately 0.1 cm/sec inflow velocity across the section. The inflow velocity corresponds to experimental observations at 1-$g_0$, 1-atm pressure. The cross section of the specimen is approximately 50 $cm^2$ and so this corresponds to a volumetric flow rate in the natural convection mode (1-$g_0$, 1-atm) of 5 $cm^3$/sec. As mentioned above, the oxidizing air will have an $O_2$ concentration arbitrarily set at 20%. When the spent gas emerges from the porous smolder specimen the flow rate will have been augmented to 9 $cm^3$/sec and the gas will contain no $O_2$. This augmentation corresponds to the stoichiometry discussed in Section 1.4 and corresponds also to measurements that have been made of the outflow gas in laboratory experiments. The fact that the $O_2$ concentration of the product gas is zero corresponds to experimental observations (Figure 5). The mixing of the emerging spent gas with the flow of replenishment oxidizing gas is supposed to create in the void volume a new mixed flow having again a 20% $O_2$ concentration. This requirement can be met, for example, by metering replenishment oxidizing gas into the void volume at a rate equal to three times the flow rate of emerging spent gas, i.e., 27 $cm^3$/sec which would contain an $O_2$ concentration of 27%. This concentration of $O_2$, when mixed with the emerging spent gas, will be reduced to 20%, the desired $O_2$ concentration in the void surrounding the porous fuel specimen. This 3:1 freshening is simply one example. For instance, if the replenishment oxidizing gas is supplied at a rate equal to 9 times that of the flow rate of emerging spent gas from the porous fuel body, the $O_2$ concentration of the replenishment gas would be 22% in order that the atmosphere in the void volume would contain 20% $O_2$. The choice of oxidizing gas supply flow rate, $O_2$ concentration, and the freshening ratio are arbitrary and can be selected to satisfy whatever design criteria is established. For example, we may choose to limit the amount of $O_2$ gas supply, in which case a lower freshening ratio would be preferred. Alternatively, we may choose to have a large supply of oxidizing gas entering the void volume so as to keep the concentration of CO and other product gases in the Combustion Facility chamber as low as possible. In this case we would choose a larger supply of oxidizing gas and a correspondingly lower percentage of $O_2$ in that supply.

As mentioned previously, an important consideration in establishing this choice is to ensure that mixing occurs with enough of the replenishment oxidizing gas to cool the atmosphere in the void. The temperature of the gas in the void exterior to the porous smolder specimen must be as low as possible in comparison with the average gas temperature within the porous smolder specimen to establish the natural convection flow pattern at reduced-g. With these considerations in mind, the choice of 3:1 freshening with a 27% concentration was made.

As for the discharge of gases from the individual cannisters to the Combustion Facility chamber, the exhaust rate must be sufficient to equal the inflow rate to the cannister from the oxidizing gas supply plus the excess flow rate established by smoldering combustion of the porous sample. The

flow circuit diagram shows that 27 $cm^3$/sec is the inflow rate from the oxidizing gas supply and the excess flow rate established by smoldering combustion is 4 $cm^3$/sec. Thus the combination, 31 $cm^3$/sec, must be withdrawn from the cannister as vitiated air. This exhaust air will obviously have an $O_2$ concentration equal to that in the void volume in the cannister. To verify and monitor these concentration levels and flow rates, it is proposed to provide each cannister with flow meters and $O_2$ concentration sensors.

Another design criterion which must be satisified is that the inflow of replenishment oxidizing gas should be so spread into the void volume so as to eliminate the possibility of direct outflow from the inflow port to the outflow port. We require the replenishment oxidizing gas to fully mix with the product gas produced by smoldering combustion of the porous sample. A cylindrical diffusing screen is provided in the cannister to spread the inflow replenishment oxidizing gas so as to achieve complete and uniform mixing. A restricting outflow screen is also provided to avoid the possibility of direct removal of the oxidizing gas prior to mixing in the void volume, i.e., offers high resistance path for flow.

Placement of the exhaust port in the reduced-g convective flow cannister is not a trivial matter. Cannister rotation coupled with the location of the exhaust port could result in a suction effect and hence influence the internal cannister fluid dynamics. Let us consider the fastest rotational speed contemplated in the experiment ca., 50 rpm. For an exhaust port located on the inboard end of the cannister, ca. 5 cm from the axis of rotation, this gives a rotational velocity of 26 cm/sec. If the air in the Combustion Facility Chamber is taken as still and not in induced rotation, this 26 cm/sec is taken as the relative air velocity. The "pitot" effect, $\Delta p_{exhaust}$, is approximately $1/2\ \rho v_\theta^2$ or 0.3 micro-atm. This is to be compared with the $\Delta p$ that will drive the replenishment gas through the cannister from inlet port to exhaust port. If the $\Delta p_{exhaust}$ is small compared with the driving $\Delta p$ then the pitot effect will be negligible and there will be no significant suction. In the design of the flow system the driving $\Delta p$ associated with the replenishment gas flow circuit must be made much larger than the buoyancy $\Delta p$ across the porous fuel body and also much greater than the $\Delta p$ caused by flow resistance through the porous fuel body. This is a necessary condition to assure the stability of the replenishment flow, to make it insensitive to variations in the pumping action of the smoldering porous body. In fact, this larger $\Delta p$ in the replenishment flow circuit would best be placed in the porous flow-spreading screens at inlet and exhaust of each cannister; by placing a larger $\Delta p$ at those two stations, the spreading of the flow in and out would be assured and made insensitive to inflow and outflow "jet streams" from the smoldering fuel body. Consider a $\Delta p$ of the replenishment circuit at least 100 times greater than the buoyancy $\Delta p$ or the pumping $\Delta p$ of the fuel body. The pumping $\Delta p$ of the porous fuel body is estimated to be 15 micro-atm. Therefore, the $\Delta p$ associated with the replenishment flow circuit should be 1500 micro-atm. This is $10^3$ times larger than the $\Delta p_{exhaust}$ and therefore suction effects are negligible.

Thus, if the replenishment flow circuit $\Delta p$ is 15 micro-atm this will assure not only the insensitivity of the flow rate to smolder pumping effects but also good flow spreading within the cannister. Furthermore, insensitivity to suction effects is also assured. This $\Delta p$ is quite manageable. We may

well find that the combined pressure drops across the flow meter and $O_2$ concentration meter in the flow circuit will be larger than 15 micro-atm and therefore we need not concern ourselves with the question of suction through the exhaust port.

## 3.2 System Electronics and Data Acquisition System

In order to generate and preserve data from the Smolder experiment, an instrumentation system including microprocessor is required to perform the following data process functions (see Figure 20).

1. Monitor the thermocouple outputs of each smolder cannister and convert to temperature (5 thermocouples per cannister;
2. Monitor the oxygen concentration within the cannister;
3. Monitor the air flow rate to the cannisters, both forced air flow rates and replenishment oxidizing gas flow rate for reduced-g natural convection smolder;
4. Confirm ignition of the smolder samples via both the output of thermocouple nearest the ignition surface and via smoke detection in each cannister;
5. Monitor motor speed of rotating assembly;
6. Monitor time (internal clock);
7. Multiplex data;
8. Digitize multiplexed data;
9. Transfer data from rotating support structure to stationary housing;
10. Store data with user-supplied recording equipment;
11. Provide scientist/astronaut with real-time status information;
12. Shut off oxidizing gas supply, purge cannisters, and cease rotation of supporting structure if excessive-temperature develops ($T > 1300$ K); and
13. Supply current to igniter elements to initiate smolder.

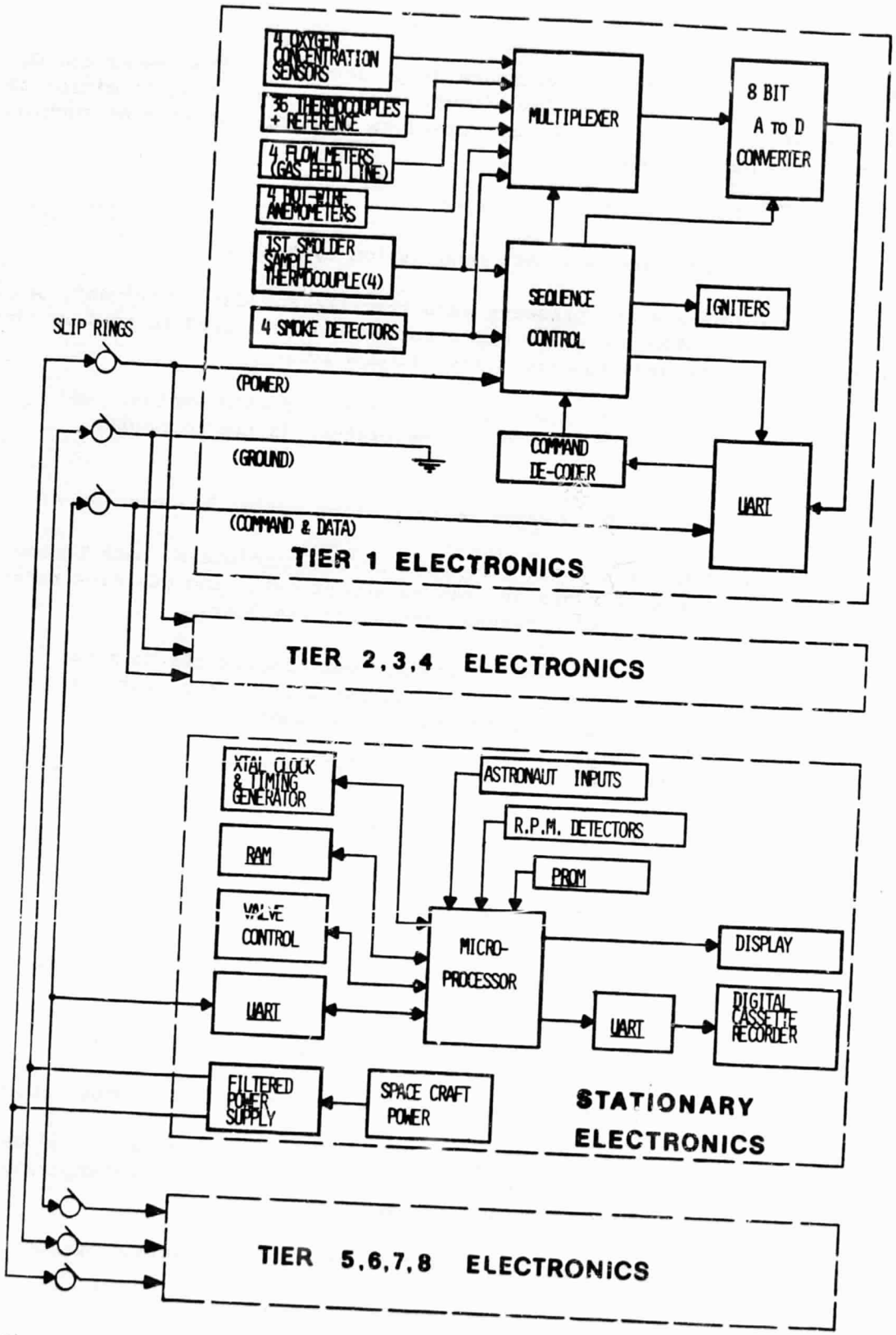


Figure 20. Schematic Diagram of System Electronics

The system, as shown in Figure 20, operates as follows:

### 3.2.1 Rotating Electronics

In each of the counter-rotating tiers (4 cannisters per tier) that will rotate during a given experimental run, analog temperature data from 40 thermocouples (6 embedded in the porous sample, 1 immediately subsurface in the sample for ignition detection, and 3 in the volume surrounding the porous sample to monitor the gas temperature; this yields 10 per cannister x 4 cannisters per tier) as well as a temperature reference, analog oxygen concentration from 4 sensors, analog gas feed line flow rate from 4 thin-film anemometers, analog output from 4 hot-wire anemometers, and the analog output from 4 smoke detectors are multiplexed into an A/D converter. The selected 8 bit multiplexer output word is serialized by a UART (Universal Asynchronous Receiver/Transmitter) whose output passes thru a slip ring on its way to the stationary electronics package. Additionally, the slip ring is used by the stationary electronics package to issue commands to various tiers of cannisters. These 8 bit serial commands are assembled by the UART in each tier and are presented to a dedicated command decoder. If the command applies to a particular tier, the sequence controller for those cannisters responds to a command decoder pulse by taking the action called for by the command. Commands will include:

1. Convert an addressed channel and transmit.
2. Convert "fire-detecting" thermocouple channel and transmit.
3. Convert thermocouple reference and transmit.
4. Transmit igniter/smoke detector status.
5. Select tier 1,2,3,4,...8.
6. Igniter <u>on</u> tier 1,2,3,4.
7. Igniter <u>off</u> tier 1,2,3,4.

In addition to implementing commands, the sequence controller monitors the smoke detector and the first thermocouple in the smolder sample for each cannister on its tier. When the outputs from the smoke detector and the first thermocouple for each cannister indicate ignition has stabilized, the sequence controller shuts off the appropriate igniter.

The multi-use of the slip ring simplifies electrical connections between the rotating data-generating electronics with the stationary, command generating and data storing electronics. In this sense it resembles a simple computer architecture and will be referred to as the Command and Data Bus.

Other electrical connections to the 4-tier bank of cannisters are power and ground via slip rings. This means that only six (6) slip rings are required for the entire system.

### 3.2.2 Stationary Electronics

The key element in the stationary electronics subsystem is a microprocessor, which is involved in every aspect of the experiment. Its responsibilities include:

1. Accept input from scientist/astronaut;
2. Set up timetable of commands to tiers and peripherals;
3. Generate timecode to keep track of elapsed time;
4. Send commands to specific tiers via UART interfacing to Command and Data Bus;
5. Accept data output from responding tier electronics via UART interfacing to Command and Data Bus;
6. Monitor key parameters in data;
7. Control and monitor motor speed;
8. Control gas flow;
9. Shut off oxidizing supply, purge chamber with $N_2$ and cease rotation of support structure if excessive temperature ($T > 1300$ K) develops, or at end of experiment;
10. Format data with sync, timecode, and status and output to tape recorder;
11. Calculate temperatures from data;

and

12. Output to scientist/astronaut's display.

### 3.2.3 Timing and Telemetry Frame Organization

A possible organization of a frame of recorded data is discussed below. The frame consists of 64 16-bit words, although the number of words can vary to accomodate the data requirements. The first word is a pseudo random sequence used for frame synchronization. This is followed by timecode whose 16 bits give almost 0.1 second granularity based on a 2 hour recording. After timecode comes 8 bits of status from upper and lower banks of tiers including selected tier, igniter status, etc. The remaining slots in the frame are devoted to multiplexed data from two tiers. Each slot contains data from a predetermined multiplexer point. Each time the last position is filled with data, the frame start over again with frame sync, and the pattern repeats continuously.

Assuming each point is sampled every 10 seconds and that there are 64 points to be monitored in each tier, the data rate is:

$$.1 \frac{\text{samples}}{\text{sec/channel}} \times \frac{8 \text{ bits}}{\text{sample}} \times \frac{64 \text{ channels}}{\text{tier}} \times 2 \text{ tiers} = 102.4 \text{ bits/sec}$$

Over two hours or recording only 740 kb of data are generated. This can easily be handled by a self-contained digital cassette recorder.

### 3.2.4 Power

Using CMOS logic (Complementary Metal Oxide Semiconductor), each tier when active should consume less than 500 mW. Therefore, for two tiers, the power requirement is 1W.

Each nonselected tier should consume less than 100 mW. Therefore, for 6 tiers, the power requirement is 0.6W.

The stationary electronics, including CMOS microprocessor should also consume less than 0.5W.

The power supply efficiency is rated at 0.70. Therefore this long duration power requirement is 4.4W.

The major power requirement is associated with the igniter coils. It should be noted that this is a short duration power requirement. From ground-based igniter experiments performed for this study, the coil resistance was found to be 2Ω and the applied coil voltage was 10.5 VAC in those cases where self-propagating smolder was established in the sample. Thus the current required was 5.25 A and therefore the power requirement for the coil was 55W. Since 8 cannisters undergo smolder combustion simultaneously, the igniter coils power requirement per run is 440W.

The power requirement (long duration) associated with the two DC stepping motors which rotate the supporting shafts is 480W.

The power requirement associated with the tape recorder is 7.9W (long duration).

Thus, during the transient ignition phase prior to a fully established, self-propagating smolder wave, the short duration power requirement is 934.4W. However, once the command is received for igniter OFF, power requirements drop substantially to 494.4W.

## 3.3 Heat Disposal System

Another critical component which we have identified was discussed in Section 2.5.2, the safety aspects associated with the heat generated by the smolder combustion process and direct exhaust of the vitiated air from the individual smolder combustion cannisters into the Combustion Facility chamber. This may require a condensation trap, a Combustion Facility cooling system, or a direct dump of the chamber atmosphere between successive runs of the Smolder Experiment. This will have to be investigated further with NASA Combustion Facility design personnel. At present, we contemplate use of the NASA-developed Chamber-Atmosphere Vent Subsystem for venting the Combustion Facility chamber of combustion products after completion of successive segments of the experiment.

## APPENDIX A: SELECTED REFERENCES


1. Alarie, Y., and Anderson, R., "Screening Proceedures for Evaluation of Toxicity of Cellular Plastics Combustion Products", Dept. of Industrial Environmental Health Sciences, Univ. of Pittsburg, First Annual Report for Products Research Committee (RP-75-2-8), Nov., 1977.

2. Andracchio, C.R. and Cochran, T.H., "Burning of Solids in Oxygen-Rich Environments in Normal and Reduced Gravity", NASA TM X-3055, May, 1974.

3. Baker, R.R., "The Kinetics of Tobacco Pyrolysis", Thermochemica Acta, 17, 1976.

4. Beitel, J.J., Pish, M.D., Herrera, W.R., Boenig, D.M., Armstrong, G.W., "Evaluate the Life and Property Hazards of Plastics and Traditional Furnishings of Completely Furnished Rooms: Vol. 1: Burning Characteristics and Off Gas Analysis", Final Report to Products Research Committee No. PR-75-1-45, Nov., 1976.

5. Benning, C.J., Plastic Foam: Vol. 1: Chemistry and Physics of Foam Formation, John Wiley and Sons, 1969.

6. Benning, C.J., Plastic Foams: Vol. II: Structure, Properties, and Applications, John Wiley and Sons, 1969.

7. Berlad, A.L. and Killory, J., "Combustion of Particulate Clouds at Reduced Gravitational Conditions", Interim Report NASA Grant NSG-3051, Feb., 1977.

8. Berlad, A.L. et al., "Study of Combustion Experiments in Space", NASA CR-134744, Nov., 1974.

9. Birky, M.M., "Toxicological Assessment of Combustion Products", Final Report to Products Research Committee, Dec., 1977.

10. Bowes, P.C. and Thomas, P.H., "Ignition and Extinction Phenomena Accompanying Oxygen-Dependent Self-Heating of Porous Bodies", C & F, 10, 1966.

11. Bowes, P.C., "Thermal Ignition in Two-Component Systems, Theoretical Model", C & F, Oct., 1969.

12. Carrier, G.F. and Fendell, F.E., "Analytic Evaluation of the ASTM E84-70 Tunnel Tests Applied to Plastics", Report of Phase I to Products Research Committee RP-75-1-43, Oct., 1976.

13. Carrier, G.F. et al., "Wind-Aided Flame Spread Along A Horizontal Fuel Slab Without Radiative Transfer", TRW Engineering Sciences Laboratory Report for Phase II, Jan. 1978.

14. Cohen, L. and Luft, N.W., "Combustion of Dust Layers in Still Air", Fuel, 34, 1955.

15. Damant, G.H., "Cigarette Induced Smoldering of Uncovered Flexible Polyurethane Foams", JFF/Consumer Product Flammability, Vol. 2, June, 1975.

16. Damant, G.H., "A Survey of Flexible Fire Retardant Polyurethane Foams", State of Calif. Flammability Research Lab Report No. SP-77-2, May, 1977.

17. Damant, G.H., "A Survey of Upholstery Fabrics and Their Flammability Characteristics", JFF/Consumer Product Flammability, Vol. 2, March, 1975.

18. De Soete, G., "Stability and Propagation of Combustion Waves in Inert Porous Media", 11th. Comb. Symposium, The Combustion Institute, Pittsburgh, PA, 1967.

19. Drake, G.L., Perkins, R.M., and Reeves, W.A., "Flame Resistant Cotton-- A Status Report", J. Fire & Flammability, Vol. 1, Jan., 1970.

20. Edelman, R.B. et al., "Analytical Study of Gravity Effects on Laminar Diffusion Flames", NASA-CR-120921, Feb., 1972.

21. Gann, R.G. and Cheng, I.T., "Flow Study of Smoldering Charcoal Combustion", Chemical Dynamics Branch, Chemistry, Naval Research Laboratory, Washington, D.C.

22. Gold, M.D., Blum, A., and Ames, B.N., "Another Flame Retardant, Tris-(1,3-Dichloro-2-Propyl)-Phosphate, and Its Expected Metabolites Are Mutagens", Science, Vol. 200, May, 1978.

23. Grayson, S.J., Green, R.J.S., Hume, J., Kumar, S., "Smoke and Toxic Gas From Burning Polyurethane Foam", QMC Industrial Research Ltd., Final Report for Product Research Committee RP-75-1-13, Sept., 1977.

24. Hilado, C.J., Flammability Handbook for Plastics, Technomic Publishing Co., Inc., 1974.

25. Kanury, A.M., "Burning of Liquid Pools in Reduced Gravity", Final Report NASA CR-13524, June, 1977.

26. Kimzey, J.H., Downs, W.R., Eldred, C.H. and Norris, C.W., "Flammability in Zero-Gravity Environment", NASA TR R-246, October, 1966.

27. Kinbara, T., Endo, H. and Sega, S., "Downward Propagation of Smoldering Combustion Through Solid Materials", 11th Combustion Symposium, Combustion Institute, Pittsburg, PA, 1967, pp. 525-531.

28. Klyachko, L.A., "Ignition of an Aggregate of Particles During Heterogeneous Reaction", Pyrodynamics, 1968, Vol. 6, pp. 29-38.

29. Knoepfler, N.B., "The Status of Research to Develop Flame Retardant Cotton Flote Products for Cushioning Applications", J. Fire & Flammability, Vol. 2, July, 1971, pp. 219-231.

30. Koizumi, M., "The Combustion of Solid Fuels in Fixed Beds", Sixth Combustion Symposium, 1956, pp. 577-583.

31. Madacsi, J.P., Neumeyer, J.P. and Knoepfler, N.B., "Boric Acid-Alcohol Treatment of Cotton Batting", Ind. Eng. Chem. Prod. Res. Dev., Vol. 15, No. 1, 1976, pp. 71-75.

32. Moussa, N.A., Toong, T.Y. and Garris, C.A., "Mechanism of Smoldering of Cellulosic Materials", Sixteenth Combustion Symposium, Combustion Institute, Pittsburg, PA, pp. 1447-1457.

33. Ohlemiller, T.J., Rogers, F.E. and Summerfield, M.,"Modeling the Generation of Toxic Gases by the Smoldering Combustion of Polyurethanes", Tenth Quarterly Progress Report to National Bureau of Standards, Feb., 1977.

34. Ohlemiller, T.J. et al., "Modeling the Generation of Toxic Gases by the Smoldering Combustion of Polyurethanes", Thirteenth Quarterly Progress Report to National Bureau of Standards, January, 1978.

35. Ortiz-Molina, M.G. et al., "Smoldering Combustion of Cellular Plastics and its Transition to Flaming or Extinguishment", Final Report to Products Research Committee (RP-76-U-3), January, 1978.

36. "The Overselling of Insulation", Consumer Reports, February, 1978.

37. Ostrach, S., "Convective Phenomena of Importance for Materials Processing in Space", Case Western Reserve University, November, 1976.

38. Palmer, K.N., "Smoldering Combustion in Dusts and Fibrous Materials", Combustion & Flame, Vol. 1, 1957, pp. 129-154.

39. Palmer, K.N. and Taylor, W., "Fire Hazards of Plastics in Furniture and Furnishings: Ignition Studies", Department of the Environment, Building Research Establishment Current Paper CP 18/75, February, 1974.

40. Palmer, K.N. and Taylor, W., "Fire Hazards of Plastics in Furniture and Furnishings: Ignition Studies", JFF/Consumer Product Flammability, Vol. 1, June, 1974, pp. 186-211.

41. Palmer, K.N. and Tonkin, P.S., "The Ignition of Dust Layers on a Hot Surface", Combustion & Flame, Vol. 1, 1957, pp. 14-18.

42. "Proceedings of the Annual Conference on Fire Research", July, 1976, Report FPP-B76-2.

43. Quintiere, J., McCaffery, B.J. and Kashiwagi, T., "A Scaling Study of a Corridor Subject to a Room Fire", ASME Report 77-HT-72, April, 1977.

44. Rogers, F.E., Ohlemiller, T.J., Kurtz, A., and Summerfield, M., "Studies of the Smoldering Combustion of Flexible Polyurethane Cushioning Materials", J. Fire & Flammibility, Vol. 9, January, 1978.

45. Shea, F.L. and Hsu, H.L., "Self-Heating Carbonaceous Materials", Ind. Eng. Chem. Prod. Res. Develop., Vol. 11, No. 2, 1972, pp. 184-187.

46. Smith, E.E. and Heibel, J.T., "Evaluating Performance of Cellular Plastics for Fire Systems", Final Report PRC Project No. RP-75-1-36.

47. Waszeciak, P.H., "Large Scale Experimental Evaluation of Release Rate Model for Predicting Fire Hazard Development in Compartments Containing Cellular Plastics", The Upjohn Co., Final 1977 Progress Report for Products Research Committee, Project No. RP-76-U-4, 1977.

48. Ohlemiller, T.J., Rogers, F.E., Kurtz, A., Bellan, J. and Summerfield, M., "Experimental and Modeling Studies of Smoldering in Flexible Polyurethanes", Two Year Summary Report, Princeton University, Department of Aerospace and Mechanical Sciences, Report No. 1337, July 15 1977.

49. Lewis, Bernard and vonElbe, Guenther, Combustion, Flames and Explosions of Gases, Second Edition, Academic Press, New York, 1961.

50. Cochran, T., Private Communication.

51 Spacelab Payload Accomodation Handbook, SLP/2104, June, 1977.